Title

Examining multiple cellular pathways at once using multiplex hextuple luciferase assaying

Alejandro Sarrion-Perdigones[1], Lyra Chang[2,3], Yezabel Gonzalez[1], Tatiana Gallego-Flores[4,&], Damian W. Young[1,2,3,5], and Koen J.T. Venken[1,2,3,5,6,*]

[1]Verna and Marrs McLean Department of Biochemistry and Molecular Biology, Baylor College of Medicine, Houston, TX, 77030, USA

[2]Department of Pharmacology and Chemical Biology, Baylor College of Medicine, Houston, TX, 77030, USA

[3]Center for Drug Discovery, Baylor College of Medicine, Houston, TX, 77030, USA

[4]Department of Molecular and Human Genetics, Baylor College of Medicine, Houston, TX, 77030, USA

[5]Dan L. Duncan Comprehensive Cancer Center, Baylor College of Medicine, Houston, TX, 77030, USA

[6]McNair Medical Institute at The Robert and Janice McNair Foundation, Baylor College of Medicine, Houston, TX, 77030, USA

[*]Correspondence:

koen.j.t.venken@gmail.com (K.J.T.V)

[&]Current address:

Max Planck Institute for Brain Research, Frankfurt am Main, 60438, Germany (T.G-F)

Abstract

Sensitive simultaneous assessment of multiple signaling pathways within the same cells requires orthogonal reporters that can assay over large dynamic ranges. Luciferases have arisen as possible genetically encoded candidates due to their sensitivity, versatility, and cost-effectiveness. Here, we expanded luciferase multiplexing in post-lysis endpoint luciferase assays from two towards six. Light emissions are distinguished by a combination of distinct substrates and emission spectra deconvolution. Using synthetic assembly cloning, all six luciferase reporter units are stitched together into one plasmid; facilitating delivery of all reporter units through a process we named solotransfection, minimizing experimental errors. We engineered a multiplex hextuple luciferase assay to probe pathway fluxes through five transcriptional response elements against a control constitutive promoter. We were able to monitor the effects of siRNA, ligand, and chemical compound treatments on their target pathways along with the four other probed cellular pathways. We demonstrate the effectiveness and adaptiveness of multiplex luciferase assaying, as well as its broad application across different research fields.

Introduction

Currently, most cell-based screening assays rely on a single measurement (e.g., enzyme inhibition or cell viability) to identify genetic or pharmacological agents that modulate the biomedical phenomenon of interest[1]. However, due to the complexity of biological systems, screens based on single biological measurements yield only limited information[2,3]. Additional screening assays must be performed to expand information content, but this often requires protracted assay development, time, and/or expense. Moreover, independently performed screens may not always be appropriately controlled, making comparative analysis across different experimental variables difficult[4,5].

Multiplexed cellular screens seek to address these limitations by measuring multiple readouts from a single screening unit simultaneously. Multiplexed biological screening from a single sample can provide a more detailed cellular signature, allowing greater perspective into the nuances which differentiate normal versus disease-associated processes[6–8]. Moreover, multiple simultaneous measurements of the same sample enable correlation and comparison between experimental variables and biological effects[9]. Some examples of multiplexed biological screening already exist that rely on fluorescent labeling. Modern flow cytometry can analyze the presence of up to 30 different antigens using labeled antibodies[10], whereas cell painting measures the presence of a multitude of morphological features of cells using a combination of fluorescent dyes and automated image analysis[11]. On the other hand, to accommodate the sensitive reporting of subtle changes in signaling pathway activities over large dynamic ranges, luciferase reporters have emerged as a promising new addition to the multiplex biological screening toolbox[12].

Luciferase reporters are widely used in biomedical research for a variety of applications, including gene expression, intracellular signaling, transcription factor characterization, receptor activity, protein folding, drug screening, analytics, and immune-based assays[12,13]. Luciferases possess many advantages over fluorescent proteins, such as higher sensitivity, wider dynamic detection range[13,14], and the absence of auto-luminescence in mammalian cells[13]. Luciferases are categorized by their enzymatic activities[13,15]: the beetle luciferases first activate their substrate (D-Luciferin and derivatives) to a product whose oxidation results in light emission, whereas the marine luciferases directly oxidize their substrate (coelenterazine, vargulin, or furimazine), generating an excited-state molecule that emits a photon. Similar to fluorescent proteins, each luciferase has a

unique emission spectrum[13,16] that enables detection of two or more luciferases simultaneously as long as the spectra are distinguishable[14,15,17,18].

Most multiplex luciferase experiments today measure the light emitted from two luciferases in succession[19]. The first, which is typically FLuc, a firefly (*Photinus pyralis)* luciferase, utilizes D-Luciferin and is used to monitor a cellular signaling event of interest. The second enzyme, often the Renilla luciferase of *Renilla reniformis* (Renilla) that uses coelenterazine[20] or the brighter NLuc (a synthetic version of the *Oplophorus gracilirostris* luciferase) that uses furimazine[21], is used as an internal control. These dual-luciferase assays allow sequential quantitative measurements of both luciferase activities in the same sample, thereby eliminating pipetting errors that could occur if measurements were performed from different samples[22]. In recent years, researchers have also developed their own (non-commercial) versions of these assays with presumably similar performance[23,24].

Inspired by the urgent need to report on subtle changes in multiple signaling pathway activities over large dynamic ranges, and the variety in substrate and spectral properties inherent to natural luciferase enzymes, we aimed to explore multiplex capabilities for luciferase-based reporter systems. Here we report multiplexed luciferase reporter assaying, capable of measuring six parameters within the same experiment, called multiplex hextuple luciferase assaying. We demonstrate the utility of this assaying by simultaneously monitoring the direct and collateral effects of introducing siRNAs, pharmaceutical drugs, and ligands targeted toward specific pathways. Our multiplex hextuple luciferase assaying is adaptable to most cellular signaling pathways of interest, cost-effective, easy to integrate into any research setting already using the dual-luciferase assay, and offers the immediate implementation in large-scale multiplex drug screening efforts.

Results

Concept of multiplex luciferase assaying

The commonly used dual-luciferase assay orthogonally detects FLuc and Renilla through sequential application of their unique substrates (D-Luciferin and coelenterazine, respectively) with proper quenching of light emission from the first enzyme before the second substrate is introduced. This is accomplished through the addition of buffers at specific time points during the assay[22]. Cells are usually co-transfected with two plasmids, one encoding a control luciferase reporter and the other encoding a pathway-specific luciferase reporter, are washed and lysed before addition of D-Luciferin and subsequent measurement of its emission. Then a quencher is added in the presence of coelenterazine, and its emission is measured (**Supplementary Figure 1a**). Based on this paradigm, we explored different options for expanding the number of luciferases catalyzing each sequential stage using readily available reagents (**Supplementary Figure 1b**).

Identification of luciferases for use in multiplex luciferase assaying

We used four criteria to identify luciferases that might be orthogonally detected in a single multiplex luciferase experiment: (**1**) preference for a single substrate over any other, and potential for luminescence quenching, (**2**) in cases where the same substrate is preferred, they must exhibit minimally overlapping emission spectra that can be distinguished by emission filters and/or mathematical computation, (**3**) stable light emission throughout the experiment to ensure high quality measurements, and (**4**) a wide dynamic range for light emission to be able to detect subtle differences in pathway activities. We assessed these four criteria for 12 luciferases: six have been reported to emit light using D-Luciferin as a substrate, one to prefer furimazine, and five to prefer coelenterazine (**Table 1**).

Criterion 1: Preference for a single substrate and luminescence quenching

To determine the substrate preference of the 12 luciferases (**Table 1**), transcriptional units containing each luciferase gene were constructed using multipartite assembly synthetic biology[25–27] (**Figure 1a**). To ensure adequate expression levels following transfection, the human cytomegalovirus (hCMV-IE1) promoter was placed upstream of each luciferase gene, and the bovine growth hormone poly-adenylation terminator

(bGHpA) was cloned downstream[28]. Vectors containing each assembled luciferase transcriptional unit were transfected into HEK293T/17 cells, and 24 hours after transfection, the absolute luciferase activity was measured after cell lysis in an endpoint experiment. Substrate preference and emission brightness of each luciferase were characterized after addition of D-Luciferin-containing buffer alone, or followed by the addition of a second buffer, containing quencher and coelenterazine. Luciferases that prefer coelenterazine as a substrate are generally brighter than those that prefer D-Luciferin so we diluted 10 times the lysates of cells expressing the coelenterazine-specific luciferases to prevent detection saturation. Six of the 12 luciferases were responsive to D-Luciferin as expected; however, some, albeit significantly reduced, luminescence levels remained for some of the D-Luciferin-specific luciferases after addition of quencher and coelenterazine. The other six enzymes were responsive to coelenterazine, and showed minimal promiscuous activity with D-Luciferin (background levels empirically set at 10^3 RLU/s) (**Figure 1b**). Although NLuc has been engineered to use the substrate furimazine, it showed strong activity with coelenterazine.

Only D-Luciferin-responsive luciferases that can be quenched down to levels similar to FLuc during the second measurement should be incorporated into multiplex luciferase assaying. The three D-Luciferin luciferases that showed the best signal quenching in terms of relative emission were ELuc (98%), FLuc (99%), and RedF (99.3=2%) (**Figure 1c**). Although the D-Luciferin signal of ELuc was only quenched to 98% of its original value, ELuc exhibited a lower absolute luminescence than FLuc and RedF (**Figure 1b**). Nevertheless, all three enzymes emitted negligible light after the addition of coelenterazine substrate compared to the background level of 10^3 RLU/s (**Figure 1b**). Our substrate specificity testing identified nine luciferases to be evaluated against the second criterion, namely three D-Luciferin-responsive luciferases (ELuc, FLuc, and RedF) and six coelenterazine-responsive luciferases (NLuc, Renilla, MetLuc, Lucia, GLuc, and GrRenilla).

Criterion 2: Ability to deconvolute emission spectra

To determine regions of minimal emission overlap between luciferases belonging to a single substrate group, emission spectra of each luciferase were recorded (**Supplementary Figure 2a**). ELuc, FLuc, and RedF have distinct emission spectra with maxima at 537 nm, 562 nm, and 617 nm, respectively that can be exploited in multiplexing experiments (**Figure 1d** and **Supplementary Figure 2b**). However, It would be impractical to attempt to distinguish between the emission spectra of the coelenterazine-responsive luciferases (NLuc,

Renilla, MetLuc, Lucia, GLuc, and GrRenilla) since Renilla, MetLuc, Lucia, and GLuc exhibit maximum emission within 7 nm of each other (482 to 487 nm) (**Figure 1e** and **Supplementary Figure 2c**). However, NLuc (462 nm) and GrRenilla (532 nm) could be readily distinguished from any of the other four, including Renilla (481 nm). Therefore, we decided to proceed with only three coelenterazine-responsive luciferases, namely NLuc, Renilla, and GrRenilla (**Figure 1f** and **Supplementary Figure 2c**).

We chose two bandpass (BP) filters to deconvolute a multiplexed luminescence measurement of the three D-Luciferin-responsive luciferases: BP515-30, which measures between 500 and 530 nm, and BP530-40, which measures between 510 and 550 nm) (**Figure 1d**). We calculated two transmission coefficients (κ) for each luciferase by dividing the light that transmits through either filter (e.g., $ELuc_{515}$ for BP515-30) by the total light emitted by each of the luciferases (e.g., $\kappa ELuc_{515} = ELuc_{515}/ELuc_{TOTAL}$) (**Supplementary Figure 3a**, **b**). Using the six transmission coefficients ($\kappa ELuc_{515}$, $\kappa FLuc_{515}$, $\kappa RedF_{515}$, $\kappa ELuc_{530}$, $\kappa FLuc_{530}$, and $\kappa RedF_{530}$) (**Supplementary Figure 3c**), we established a mathematical model (i.e., simultaneous equations consisting of three equations and three variables) to determine the contribution of the three individual luciferases to the experimental luminescence value recorded with the BP515-30 ($Light_{515}$) and BP530-40 filters ($Light_{530}$), as well as without any filter ($Light_{TOTAL}$) (**Supplementary Figure 4a**). Using this model, total luminescence was calculated for ELuc, FLuc, and RedF (**Supplementary Figure 4b**).

We used two alternative BP filters to specifically separate the spectra of coelenterazine-responsive luciferases due to the similar transmission coefficients when BP515-30 and BP530-40 are used for NLuc and Renilla: BP410-80, which measures between 370 and 450 nm, and BP570-100, which measures between 520 and 620 nm (**Figure 1f**). Again, we calculated the transmission coefficients (κ) by dividing the light transmitted from each luciferase through both filters ($NLuc_{410}$, $Renilla_{410}$, and $GrRenilla_{410}$, as well as $NLuc_{570}$, $Renilla_{570}$, and $GrRenilla_{570}$) by the total light emitted from each luciferase ($NLuc_{TOTAL}$, $Renilla_{TOTAL}$, and $GrRenilla_{TOTAL}$) (**Supplementary Figure 3a** and **d**). Using the six transmission coefficients for this series ($\kappa NLuc_{410}$, $\kappa Renilla_{410}$, $\kappa GrRenilla_{410,}$ $\kappa NLuc_{570}$, $\kappa Renilla_{570}$, and $\kappa GrRenilla_{570}$) (**Supplementary Figure 3e**), we established a second mathematical model to determine the contribution of the three individual coelenterazine-responsive luciferases to the experimental luminescence value recorded with the BP410-80 ($Light_{410}$) and BP570-100 filters ($Light_{570}$), as well as without any filter ($Light_{TOTAL}$) (**Supplementary Figure 4c**). Using this

second model, we calculated the total luminescence for NLuc, Renilla, and GrRenilla (**Supplementary Figure 4d**).

We expressed the six luciferases in different human cell lines (A549, MCF7, MDA-MB-231, and SK-BR-3) to determine the consistency of the transmission coefficients (**Supplementary Table 1**). Data from these experiments demonstrate that the transmission coefficients are reproducible between cell lines (**Supplementary Table 1**). Nonetheless, re-evaluation of the transmission coefficients in every experimental setup is highly recommended before performing experimental assays since changes in pH or temperature can slightly affect the luciferase emission spectra and therefore the transmission coefficient values[29].

Criterion 3: Stable light emission throughout the experiment

To determine the best time window to perform the experiment, light emission was recorded for 180 seconds after substrate injection. ELuc, FLuc, and RedF are glow-type luciferases that exhibit a prolonged stable signal but with lower intensity (**Figure 1g**, left, and **Supplementary Figure 5a**, **b-d**, top, and **e**, left). ELuc plateaued after 12 seconds and remained very stable over time, but FLuc and RedF required more time for the luminescence signal to stabilize. In fact, FLuc emission did not plateau in the 180 seconds after substrate injection despite a slight change in signal after 25 seconds. RedF was very stable between 20 and 70 seconds and then decayed slowly. The optimal period for measuring these luciferases was determined to be at 30 seconds post-injection (**Figure 1g**, right, and **Supplementary Figure 5e**, right). Since the intensity of D-Luciferin-responsive luciferases is lower, we proceeded with 2-second measurement windows.

In contrast, NLuc, Renilla, and GrRenilla are flash-type luciferases that elicit a stronger yet shorter-lived signal (**Figure 1h**, left, and **Supplementary Figure 6a-d**, and **e**, left). We determined that the best window for measuring these luciferases was at 7 seconds post-injection because the luminescence of NLuc decays quickly after 10 seconds (**Figure 1h**, right, and **Supplementary Figure 6e**, right). Due to their strong luminescence, only 1-second measurements were needed for these luciferases.

It is important to note that quenching kinetics of the D-Luciferin-responsive luciferases must be fast to minimize background during the second step of the assay. Fortunately, the luminescence dropped to background levels within 4 seconds post-injection and did not affect measurements of the coelenterazine-responsive luciferases (**Supplementary Figure 5b-d**, bottom). Based on all of these results, we established a

protocol for multiplex hextuple luciferase assaying (**Figure 1i** and **Supplementary Figure 7**). Briefly, cells are washed and lysed at 24 to 48 hours post-transfection of luciferase reporter plasmids. Cell lysates are then incubated with D-Luciferin substrate for 30 seconds before total light, BP515-30-filtered light, and BP530-40-filtered light are measured serially (2 seconds/measurement). Quencher and coelenterazine substrate are then added, and cell lysates are incubated for 7 seconds before BP510-80-filtered, BP570-100-filtered, and total light are measured serially (1 second/measurement). At the end of this protocol, six luminescence values are available for further analysis.

Criterion 4: A wide dynamic range of light emission

Next, we sought to determine whether simultaneous quantification of three luciferases is possible across a wide dynamic range. To accomplish this, we determined the quantitative relationships between the three luciferases within each group using serial dilutions of the cell lysates. We transfected ELuc, FLuc, or RedF-expressing vectors into HEK293/T17 cells. Seven cell lysate mixtures with defined volume ratios (0:100, 20:80, 40:60, 50:50, 60:40, 80:20, and 100:0 ratios) of two of the three luciferases (e.g., ELuc and FLuc) were prepared in addition to lysates consisting of an equal volume of the third luciferase (e.g., RedF). After addition of D-Luciferin substrate to each mixture, total light, BP515-30-filtered light, and BP530-40-filtered light were measured (**Figure 2a**, and **Supplementary Figure 8a**). The deconvoluted luminescence signals of ELuc and FLuc were in proportion with their relative amounts added to the mixture and their respective regression curves showed excellent linearity (r^2_{ELuc} = 0.9982 and r^2_{FLuc} = 0.9998) (**Figure 2b** and **Supplementary Figure 8b**, left). The RedF luciferase signal was constant in all the samples, and the slope of this regression did not significantly differ from zero as expected. We performed a similar experimental setup for the two other combinations, resulting in similar quality regression lines when FLuc and RedF were varied and ELuc was kept constant (r^2_{FLuc} = 0.9906 and r^2_{RedF} = 0.9993) (**Figure 2c** and **Supplementary Figure 8c**, left), as well as when ELuc and RedF were varied and FLuc was kept constant (r^2_{ELuc} = 0.9979 and r^2_{RedF} = 0.9979) (**Figure 2d** and **Supplementary Figure 8d**, left). Next, we determined the dynamic range of luciferase separation using serial dilutions of the seven mixtures and found it to be stable over at least two orders of magnitude spanning from >10^6 to ≥10^4 RLU/s for the D-Luciferin-responsive luciferases, demonstrating that excellent linearity was

maintained (**Supplementary Figure 8b-d**). Importantly, the transmission coefficients did not change in the proposed experimental dynamic range (**Supplementary Table 2**).

We performed a similar experimental setup for the coelenterazine-responsive luciferases, adding the appropriate quencher and coelelenterazine solution (**Figure 2e** and **Supplementary Figure 9a**). These experiments showed good linearity in all possible combinations: when NLuc and Renilla were varied and GrRenilla was kept constant (r^2_{NLuc} = 0.9868 and $r^2_{Renilla}$ = 0.9979) (**Figure 2f** and **Supplementary Figure 9b**, left), when Renilla and GrRenilla were varied and NLuc was kept constant (*i.e.*, $r^2_{Renilla}$ = 0.9825 and $r^2_{GrRenilla}$ = 0.9996) (**Figure 2g** and **Supplementary Figure 9c**, left), as well as when NLuc and GrRenilla were varied and Renilla was kept constant (r^2_{NLuc} = 0.9976 and $r^2_{GrRenilla}$ = 0.9877) (**Figure 2h** and **Supplementary Figure 9d**, left). Similar to the D-Luciferin-luciferases, the dynamic range of separation of these luciferases was stable over at least two orders of magnitude spanning from >10^7 to ≥10^5 RLU/s, demonstrating that linearity was maintained (**Supplementary Figure 9b-d**). Again, the transmission coefficients for the coelenterazine-luciferases did not change in the proposed experimental dynamic range either (**Supplementary Table 2**).

Collectively, these results indicate that the activities of the three enzymes within each luciferase group can be determined accurately and deconvoluted with a dynamic range of >10^6 to ≥10^4 RLU/s for the D-Luciferin-luciferases and >10^7 to ≥10^5 RLU/s for the coelenterazine luciferases (**Figure 1i** and **Supplementary Figure 7**).

Implementation of synthetic assembly cloning to favor stoichiometric cellular uptake of each luciferase reporter by solotransfection

We implemented a synthetic assembly cloning approach to generate multigenic vectors in a rapid and adaptable fashion to favor stoichiometric cellular uptake of each reporter in each transfected cell. As a proof of concept, we designed a multiplex hextuple luciferase vector to simultaneously probe transcriptional signaling through c-Myc, NF-κβ, TGF-β, p53, and MAPK/JNK response elements (RE) against a control constitutive promoter, the hCMV-IE1 promoter[28]. We tested several constitutive promoters (hCMV-IE1, hEF1A, PGK, and SV40), under varying experimental conditions and found that the hCMV-IE1 promoter was the most consistent in expression levels amongst different cell lines (data not shown). Synthetic assemblies were performed using the GoldenBraid 2.0 platform[25,26], which stitches DNA fragments together using Type IIs restriction enzymes

and unique 4-base pair overhangs to direct the order of assembly of the different fragments (**Figure 3a** and

Supplementary Figure 10a). The DNA fragments used in this work were: (**i**) the hCMV-IE1 promoter[28] (**ii**)

tandem repeats of different DNA operator elements that report on c-Myc (5xE-box_RE), NF-κβ (5xNF-κβ_RE),

TGF-β (4xTGF-β_RE), p53 (2xp53_RE), and MAPK/JNK signaling (6xAP-1_RE) (**Supplementary Table 3**),

(**iii**) a mini-promoter (MiniP) that was previously shown to be inactive without added enhancer elements[30], (**iv**)

luciferase-coding DNA sequences (ELuc, FLuc, RedF, NLuc, Renilla, or GrRenilla), (**v**) a strong transcriptional

terminator (the bovine growth hormone polyadenylation signal)[28], and (**vi**) a transcription blocker[31] (**Figure 3b**).

The control luciferase reporter unit consisted of the hCMV-IE1 promoter, ELuc, and bGH polyadenylation

signal (**Figure 3c**, **Supplementary Figure 10b**, and **Supplementary Table 4**).

Different luciferase combinations were pilot-tested to ensure good measurements in multiplex luciferase

assaying, NLuc was the brightest among the luciferases described here and therefore our first choice to be

used as the standard, since the brightest of the FLuc/Renilla pair is typically used as normalization agent.

However, when any of the coelenterazine-responsive luciferases were used as the standard, high experimental

errors between biological replicates were observed after emission values for the individual luciferases were

deconvoluted from the mix (**Supplementary Figure 11**). Our previous results suggested that signal separation

is more optimal when all luciferases emit light within a similar range (**Figure 2a**-**h**, **Supplementary Figure 8a**-

d, and **Supplementary Figure 9a**-**d**). The luminescence generated by the hCMV-IE1:ELuc:bGHpA construct

in HEK293T/17 cells ranged between 10^5 and 10^6 RLU/s, which was the observed emission range of

luciferases fused to response elements of signaling pathways in initial experiments (data not shown). We

tested ELuc, FLuc, and RedF as possible references for normalization in the multigenic vector

(**Supplementary Figure 12a**). ELuc exhibited good reproducibility (**Supplementary Figure 12b-d**), and was

the only luciferase found to be useful as a normalization standard in multiplex luciferase assaying.

Next, we built pathway reporters from specific DNA operator elements (e.g., 5xE-boxes to detect c-Myc

signaling), the miniP mini-promoter, one of five remaining luciferases (e.g., Renilla), and the

bGH polyadenylation signal (**Figure 3d** and **Supplementary Figure 10c**). We insulated the pathway reporters

by adding a transcription blocker[31] (**Figure 3e** and **Supplementary Figure 10d**). Five insulated response

pathway reporter units and the control reporter unit were sequentially stitched together to generate the

multiplex hextuple luciferase reporter (**Figure 3f** and **Supplementary Figure 13**). Using this construct, we can

simultaneously monitor changes in the activity of five signaling pathways by measuring the light emission from the individual luciferases relative to the control luciferase driven by the constitutive promoter. We performed Sanger sequencing, restriction enzyme fingerprinting, and uncut supercoiled conformation analysis to ensure that every plasmid generated was correct, intact, and stable (**Figure 3g-h** and **Supplementary Figure 14**).

To distinguish classical "cotransfection" methods from that which introduces multiple genetic elements carried on a single plasmid constructed by synthetic assembly cloning, we propose the new term "solotransfection". Our multiplex construct incorporates all six transcription units on the same vector, ensuring an identical copy number of each unit in every transfected cell. In contrast, the classical cotransfection method relies on equal plasmid uptake by every cell, generating greater variability between (**Figure 4a**). We compared both transfection methods by solotransfecting the multigenic vector in one sample (150 ng of the multiplex vector, which corresponds to 1.09×10^{10} molecules) and cotransfecting a similar number of molecules for each of the six individual plasmids in a second cell sample (**Supplementary Table 5**). Luciferase measurements were performed at 24 hours post-transfection and absolute luminescence values for the six luciferases (n=4) were plotted for both methods in three different cell lines (A549, HEK293T/17, and SK-BR-3) (**Figure 4b-d**). The trend displayed by the six luciferases was similar for both approaches across the three cell lines. However, luminescence in the solotransfection experiment exhibited a smaller coefficient of variation (%CV), demonstrating that solotransfection of all reporter units assembled onto one vector leads to more consistent results than cotransfection of six individual plasmids expressing a single reporter unit. This trend was not only observed while comparing cotransfection versus solotransfection of all six transcriptional units. Cotransfecting even just two, or three, four, five and again six transcriptional units, resulted in larger coefficients of variations compared to solotransfection of the six transcriptional units (**Supplementary Figure 16a**). This indicates that, besides simplifying the transfection process, the overall error of the experiment will be reduced when all units are solotransfected, ensuring robust experimental rigor and reproducibility.

Collateral effects of siRNA knockdown is revealed by multiplex luciferase assaying

To test our multiplex luciferase approach, we analyzed the effects of previously verified siRNA knockdown on key upstream pathway-associated transcriptional response elements included in the multiple luciferase vector (**Supplementary Table 6**). We treated A549 cells in 96-well plates with 10 nM siRNA (alone or in

combination) and incubated them for 24 hours prior to solotransfection with the multiplex luciferase vector. After incubation for an additional 24 hours, cells were lysed and the multiplex luciferase assay was performed as described (**Figure 5a**). In parallel, A549 cells were similarly treated in 6-well plates, followed by extraction of mRNA and quantitative PCR (qPCR) to determine the effect of each siRNA on transcript levels of downstream genes regulated by each of the five signaling pathways: *CDKN1A*/*p21* and *BAX1* (p53 pathway), *DAPK1* and *SMAD7* (TGF-β pathway), *IL6*, *BCL-X* and *CCL2* (NF-κβ pathway), *E2F1* and *TERT* (c-Myc pathway), and *MMP1* and *VEGFD* (MAPK/JNK pathway). qPCR analysis confirmed that all siRNAs reduced the target mRNA level up to 16-fold (see **Supplementary Figure 16a**-**e** and **Supplementary Table 7**). It must be noted that the genes that were selected as downstream indicators of pathway modulation are likely regulated by multiple transcription factors due to crosstalk between the different pathways so not all genes related to a signaling pathway follow the downstream trend reported by synthetic response elements. For instance, *CDKN1A* transcription is coregulated positively by both the p53 and TGF-β pathways[32], whereas *VEGFD* transcription is downregulated by TGF-β[33], but upregulated by MAPK/JNK[34].

The multiplex luciferase assay showed that knockdown of *TP53* transcript levels resulted in a 4-fold reduction in p53 pathway activity with significant collateral repression of the NF-κβ and MAPK/JNK pathways and activation of the c-Myc pathways. We did not observe significant changes in the TGF-β pathway (**Figure 5b**, left). These results are consistent with data generated from qPCR analysis of downstream genes associated with these pathways: *CDKN1A*, *BAX1*, *IL6*, *BCL-X*, *CCL2*, and *MMP1* were downregulated, while *E2F1* and *TERT* were upregulated. Only *VEGFD* did not exhibit any significant changes in transcript level following siRNA treatment (**Figure 5b**, right). These results were corroborated when we assayed *TP53* silencing using vectors that include just one pathway reporter at a time (see **Supplementary Figure 16b, c**).

On the other hand, knockdown of *SMAD2* transcript levels resulted in a 1.5-fold reduction of TGF-β pathway activity, but only when they were previously stimulated with recombinant TGB-β protein to stimulate a pathway that demonstrates otherwise basal activity levels. Under these conditions, we also detected significant collateral downregulation of the c-Myc and upregulation of the MAPK/JNK pathway activities (**Figure 5c**, right, **Supplemental Figure 16d**). These results correlate with the data obtained by qPCR of downstream genes associated with these pathways: *SMAD7*, *E2F1*, *TERT*, *MMP1* and *VEGFD* (**Figure 5c**, left).

Furthermore, according to the multiplex luciferase assay, combined knockdown of *RELA*/*p65* and *NFKB1*/*p50* transcript levels resulted in a 2-fold reduction in NF-κβ pathway activity, as well as collateral repression of TGF-β and activation of the p53 and c-Myc pathways. We did not detect significant change in pathway activity for the MAPK/JNK pathway (**Figure 5c**, left and **Supplementary Figure 16e**). These results are similar to those obtained by qPCR analysis of downstream genes. In particular, *IL6*, *CCL2*, and *DAPK1* were downregulated, while *CDKN1A*, *BAX1*, and *E2F1* were upregulated. Exceptions were *SMAD7* and *TERT* and expression of these transcripts were not altered significantly (**Figure 5c**, right).

Downregulation of *MYC* transcript levels resulted in a 2-fold reduction of c-Myc pathway activity, as well as collateral repression of the TGF-β and upregulation of the NF-κβ and MAPK/JNK pathway activities (**Figure 5d**, left and **Supplementary Figure 16f**). A similar outcome was demonstrated by qPCR: *E2F1*, *TERT*, and *DAPK1* were downregulated, while *IL6*, *BCL-X*, *CCL2*, *MMP1*, and *VEGFD* were upregulated. Transcript levels of *SMAD7* were not significantly changed (**Figure 5d**, right).

Finally, silencing of the AP1 complex using combined siRNAs against *JUN* and *FOS* resulted in a 1.1-fold reduction of MAPK/JNK pathway activity, accompanied by strong downregulation of p53 and c-Myc pathway activities (1.3- and 0.5-fold, respectively) (**Figure 5e**, left and **Supplementary Figure 16g**). Similar effects were demonstrated by qPCR as *MMP1*, *CDKN1A*, *BAX1*, *E2F1*, *TERT*, *MMP1* and *VEGFD* were all found to be downregulated. (**Figure 5e**, right).

Assessing the effects of pharmaceutical and ligand treatment on multiple signaling pathway activation using multiplex luciferase assaying

To further confirm the utility of this new approach, we analyzed the effects of pharmaceuticals (Nutlin-3 and Chetomin) and ligands (TGF-β) that perturb two of the signaling pathways included in the multiplex luciferase vector. Nutlin-3 is a small molecule that selectively activates the p53 pathway by blocking MDM2 repression of TP53. Cells with wild-type (WT) TP53 function (e.g., ZR-75-1 and MCF7 cell lines) exhibit TP53 activation after Nutlin-3 treatment, followed by cell cycle arrest, apoptosis, and senescence[35] (**Figure 6a**, left). In contrast, TP53 cannot be activated in cell lines that carry loss-of-function *TP53* mutations (e.g., R280K mutation in MDA-MB-231 cells) or null mutations (e.g., MDA-MB-157). (**Figure 6a**, right). Adding Nutlin-3 during the transfection procedure results in potent, dose-dependent activation of the p53 pathway in ZR-75-1 (**Figure 6b**)

and MCF7 (**Figure 6c**) cells, which is consistent with results produced by qPCR analysis of *BAX1* and *CDKN1A* (**Supplementary Figure 17a-b**). Examples of collateral effects observed after Nutlin-3 treatment include c-Myc pathway repression and MAPK/JNK pathway activation in both ZR-75-1 and MCF-7 cells. Strong TGF-β or NF-κβ repression was observed only in MCF-7 or ZR-75-1 cells, respectively. There is agreement between luciferase measurements and qPCR results for most pathways and downstream genes. Only the NF-κβ pathway exhibited contradictory results in response to Nutlin-3; luciferase measurements indicated downregulation, whereas qPCR results indicated upregulation of the downstream genes for the ZR-75-1 line. (**Supplementary Figure 17a-b**). As expected, p53 pathway activation was not observed after Nutlin-3 treatment of MDA-MB-231 (**Figure 6d**) or MDA-MB-157 (**Figure 6e**) cells, either by luciferase reporters or by qPCR analysis of genes regulated by TP53 (**Supplementary Figure 17c-d**). An example of a clear collateral effect observed in both cell lines is the repression of TGF-β pathway activity. Previously, it was reported that the chemical Pifithrin-α, a well-known TP53 inhibitor, inhibits collaterally the activity of FLuc, both *in vitro* and *in vivo*, emphasizing caution when effects on reporter gene expression are being investigated, after the addition of any novel chemical compound[36]. Hence, to exclude the possibility that Nutlin-3 treatment has any effect on one or more of the luciferase activities, we assayed the drug against each constitutively expressed luciferase. As shown, Nutlin-3 treatment had no significant effect on any of the luciferase activities, while Pifithrin-α solely inhibited the activity of FLuc (**Supplementary Figure 18**).

Interestingly, a small molecule called Chetomin can rescue p53 pathway activation in some *TP53* mutant cells lines[37]. SK-BR-3 cells, which carry a homozygous *TP53* point mutation (R175H), do not show p53 pathway activation upon Nutlin-3 treatment, similar to other *TP53* mutant or null cell lines. However, in the presence of Chetomin, the TP53[R175H] protein gets reactivated and restores a WT-like function (**Figure 6f**). As shown, adding 10 μM Nutlin-3 alone to SK-BR-3 cells did not alter p53 pathway activity, but repressed the TGF-β pathway and activated the c-Myc and MAPK/JNK pathways (**Figure 6g**). Adding 150 nM Chetomin alone resulted in several changes: p53 pathway became activated, c-Myc pathway became more activated, NF-κβ and MAPK/JNK pathways were repressed, and TGF-β pathway was no longer repressed (**Figure 6g**). The addition of 10 μM Nutlin-3 with 150 nM Chetomin produced an outcome that was similar to adding Chetomin alone, except that p53 pathway activity was further enhanced, and NF-κβ pathway activity was further repressed. The MAPK/JNK pathway repression was neutralized (**Figure 6g**). The luciferase

measurements were confirmed by qPCR analysis of downstream genes (**Supplementary Figure 19**), while the non-specific inhibition effects of Chetomin on the six luciferase activities was excluded by assaying the drug against each constitutively-expressed luciferase (**Supplementary Figure 18**).

Finally, we performed the multiplex luciferase assay to examine the effects of recombinant TGF-β on TGF-β-responsive (MDA-MB-231 and MCF7) or insensitive (ZR-75-1 and SK-BR-3) breast cancer lines (**Figure 6h**). Adding 5 ng/mL of recombinant TGF-β at 16 hours post-transfection resulted in different responses among the four cell lines, 6 hours after ligand addition. MDA-MB-231 and MCF7 cells demonstrated significant activation of TGF-β pathway activity **(Figure 6i-j)**, while ZR-75-1 and SK-BR-3 cells were unaffected (**Figure 6k-l**). An additional collateral effect, namely slight downregulation of the c-Myc pathway, was observed in MDA-MB-231 cells (**Figure 6i**). All of these observations were confirmed by qPCR analysis of downstream genes with the exception of *CDKN1A*, *IL6*, and *CCL2*, which were upregulated (**Supplementary Figure 20a-d**). These data are consistent with previous findings in other cell lines that demonstrated the presence of SMAD-binding elements within the *CDKN1A*[32] and *CCL2*[38] promoters or direct crosstalk between the TGF-β and NF-κβ signaling pathways from the *IL6* promoter[39,40]. Moreover, recombinant TGF-β did not demonstrate any significant effect on one or more of the luciferase activities by assaying the drug against each constitutively expressed luciferase (**Supplementary Figure 18**).

Discussion

Dual-luciferase assays are widely employed throughout biomedical research fields[12,13]. Despite plentiful advances in the luminescence field[13], the number of luciferases that can be detected simultaneously in a single experiment has remained limited. One innovation toward multiplexing is the implementation of two luciferases that produce distinguishable emission spectra, using a single[41] or separate, orthogonally acting[14] substrates. Another innovation incorporates the use of two luciferases with emissions that can be deduced from partially overlapping substrate usage, *i.e.*, one substrate is used by both luciferases and a second substrate is used by only one[42]. More advanced innovations toward multiplexing allow for the simultaneous detection of three luciferases with activities that can be spectrally distinguished using appropriate emission filters after the addition of one[18] or more substrates[43]. Alternatively, three luciferases that each use a unique substrate have been used to monitor three distinct cellular phenomena *in vitro*[44] or, sequentially, *in vivo*[45]. Thus, currently the maximum number of luciferases that can be measured simultaneously is only three. Since applications of these tri-luciferase detection methods have not been broadly implemented, it is fair to say that today luciferase multiplexing is limited to two.

Here we demonstrate an approach that enables the detection of six luciferases simultaneously in a single endpoint post-lysis experiment using standard, well characterized, reagents. Our novel hextuple reporter assaying method multiplexes six luciferase enzymes whose activities can be uniquely determined by combining orthogonal substrate usage, selective quenching of the luminescence, and spectral decomposition. The assay enables the examination of five cellular activities against a constitutively active reporter. Successful implementation of the assay requires that appropriate filters and readout times are used, and that luminescences are within the dynamic range of the assay, which spans from $>10^6$ to $\geq 10^4$ RLU/s for the D-Luciferin luciferases and from $>10^7$ to $\geq 10^5$ RLU/s for the coelenterazine luciferases. To facilitate this assaying, we also established a versatile and adaptable cloning pipeline to generate a multigenic vector that contains all six luciferase reporter units. While we incorporated reporter elements for five specific cellular pathways, any other pathway could easily be included depending on the biomedical problem to be probed. Moreover, this work demonstrates that solotransfection of a single multi-reporter is favored over cotransfection of six individual vectors, decreasing variability between biological replicates and providing an additional level of experimental control. In conclusion, our approach reported here allows for simultaneous readout of

transcriptional activity of five cellular activities providing a much deeper understanding of cellular pathway activities of interest.

The development of a new technology or the substantial expansion of an existing technology always raises concerns and limitations. One concern of our method may be the size of the plasmid used (13.4 kb), potentially limiting its applicability using hard to transform cell lines. However, Lipofectamine 3000-mediated transfection, the transformation method used in the present study, can be substituted for by any other method, including many other lipofection or chemical transfection methods, as well as electroporation, sonoporation, and viral transduction methods[46]. Alternatively, stable cell line clones can be isolated by selection after any of the above mentioned transformation methods, previously demonstrated to work for plasmids up to hundreds of kilobases in size, including bacterial artificial chromosomes[47–49]. To reduce variability of measurements as much as possible, stable cell lines could be generated by the targeted integration of all multiplex reporters at the same defined site in the genome, such as a safe harbor site[50], resulting in the neutralization of genomic position effects. Cells with such genome-integrated luciferase reporters can then be further used to explore luciferase multiplexing towards *in vivo* bioluminescence applications [51–53]. Another concern may be potential cross-talk between the reporters integrated into the same plasmid by synthetic biology. In our multiplex reporter construct, besides a transcription terminator downstream of each transcriptional reporter unit, we have also included a well-characterized transcription blocker element in between each of the units (*i.e.*, a synthetic polyA terminator and the RNA polymerase II transcriptional pause signal from the human α2 globin gene), to prevent transcriptional interference between different pathway-responsive luciferase transcriptional units[31]. In this work, we demonstrate that cross-talk between the different response elements located on the same plasmid couldn't be observed. Also, experiments should exclude the possibility that the tested drugs may inhibit the enzymatic activities of one or more luciferases in the assay, as previously reported for Pifithrin-α[36]. This becomes especially important in high-throughput drug screens, where numerous candidates will be identified of which some may result in possible false positive hits due to interference with luciferase activity[36,54,55], careful follow-up studies, as illustrated in this work, should be performed to exclude interference of isolated compounds on luciferase activity. Finally, while the current study involves intracellularly-localized luciferases, endpoint post-lysis experimentation only allows for a single multiplex measurement. One potential solution is the adding of a membrane export signal to each luciferase to help their extracellular secretion[56]; combining this approach with

the generation of stably integrated cell line clones, longitudinal reporter studies and multiple multiplex measurements become possible by taking small media samples for analysis at defined points over time.

In future work, more luciferases could be integrated to expand the capabilities of this assay. Approaches to accomplish this include molecular modification of existing luciferases into regions of emission spectra not yet covered by the D-Luciferin- or coelenterazine-responsive luciferases or investigation of luciferases that utilize other substrates (such as vargulin and furimazine)[13,51]. Additional luciferases can be easily incorporated in our multiplex pipeline by synthetic assembly[25–27]. It is noteworthy to mention that plate reader hardware currently only provides two injectors and therefore only accommodates the simultaneous use of two luciferase substrates. We hope that this work will stimulate plate reader hardware improvements to accommodate the implementation of three or more luciferase substrates in the near future. Alternatively, compatibility with other non-luciferase reporters could be explored to expand the assay capabilities even further.

Besides applications in cancer research, as demonstrated here, hextuple luciferase assaying can be used to study other cellular pathways or complex diseases. By using the hextuple luciferase reporter system, it will be possible to simultaneously monitor the activities of five nuclear receptors by placing the specific regulatory elements upstream of five different luciferases[57], making it possible to measure nuclear receptor cross-reactivities, determine natural ligand specificity, and screen for agonists and antagonists at the same time. Hextuple luciferase assaying could also be used to monitor five known transcription factor activities downstream of the insulin receptor signaling pathway[58], enabling an investigator to probe environmental factors and pharmaceuticals affecting insulin sensitivity in different cell types. The assay could be tailored to study the innate immune responses of host cells during viral infection, which is predominantly mediated by three types of receptors[59]. Furthermore, measuring the activities of transcription factors acting downstream of these pathways would reveal correlations between viral susceptibility and the innate immune response. Multiplex luciferase assays will also be tremendously helpful in the quantification and comparison of genetic regions for synthetic biology applications both *in vitro* and, with some adaptations *in vivo*. Current methods to assess these regions and enable predictive engineering of synthetic genetic circuits rely mostly on dual-luciferase assay outputs[60]; therefore, implementing multiplex luciferase assay approaches will increase the rate and reliability of these assessments. In conclusion, the dual- luciferase reporter system has become a staple of modern biological research and the necessary hardware has become reasonably ubiquitous. Multiplexed

versions will likely be adopted across a diversity of biological disciplines, and the need for more information-rich experimental designs will lead to applications beyond the traditional dual-luciferase system.

Methods

DNA synthesis, synthetic assembly, and molecular biology

Molecular biology experiments, including plasmid maps and *in silico* experimentation, were designed and generated using SnapGene software (http://www.snapgene.com/products/snapgene/) (GSL Biotech LLC). Synthetic DNA assemblies were performed using the GoldenBraid 2.0 DNA assembly framework, a Type IIs restriction enzyme cloning method based on the use of two levels of plasmids (Alpha and Omega) that can be combined in successive rounds of assemblies (going from Alpha to Omega, back to Alpha to Omega, and so on) to create a perpetual loop allowing for virtually indefinite growth of assemblies (limited only by vector backbone properties and the stability of insert DNA). GoldenBraid 2.0 allows a convenient way to combine multiple transcriptional units into a single DNA strand[25–27]. Synthetic DNA was obtained as oligonucleotides (Sigma-Aldrich), DNA fragments or blocks (IDT and Eurofins Genomics), or cloned DNA (Twist Bioscience). All DNA blocks were transferred to the domestication vector pUPD[25,26], or a new domestication vector generated for this project (pUPD3) (**Supplementary Figure 21a** and **b**). All domestication experiments were confirmed by agarose gel DNA electrophoresis after restriction enzyme digestion to expose diagnostic DNA bands of specific lengths (restriction enzymes were purchased from New England BioLabs), as well as control uncut plasmid to eliminate unwanted multimeric assemblies. In addition, we built high-copy vectors with a ColE1 origin of replication (pColE1_Alpha1, pColE1_Alpha2, pColE1_Omega1, and pColE1_Omega2), allowing for GoldenBraid 2.0-based stitching of insert assemblies up to about 25 kb (**Supplementary Table 4**). The multi-luciferase reporter plasmid was built with successive rounds of assembly (**Figure 3**), and included five luciferases under the control of pathway-specific transcriptional response elements (**Supplementary Table 4**) and a sixth luciferase (ELuc) that served as the internal standard for normalization purposes. All assembly steps were performed in one-pot-one-step reactions (**Figure 3c-e**, **Supplementary Figure 10b-d**, and **Supplementary Figure 13**)[25,26]. To summarize, 75 ng of the destination vector and 75 ng of each of the parts to be assembled were mixed with 1 μL of the appropriate restriction enzyme (BsaI or BsmBI, New England BioLabs), 1 μL of T4 Ligase, and 1 μL of the Ligase 10x Buffer (Promega) in a final volume of 10 μL. Reactions were set up in a thermocycler with 25 cycles of digestion/ligation reactions (2' at 37°C, 5' at 16°C). Two μL of the reaction were transformed into DH10β chemocompetent *E. coli* cells (Thermo Fisher Scientific) and

positive clones were selected on solid media containing X-Gal and the appropriate antibiotic: 100 μg mL^{-1} ampicillin for GBParts assembled in pUPD, 30 μg mL^{-1} kanamycin for Alpha destination vectors, and 12.5 μg mL^{-1} chloramphenicol for the GBParts assembled in pUPD3 and Omega destination vectors. Only white colonies were pursued further; blue colonies are reconstituted destination vectors. Plasmid DNA from white colonies was extracted using the ChargeSwitch-Pro Plasmid Miniprep Kit (Thermo Fisher Scientific). Assemblies were confirmed by agarose gel DNA electrophoresis after restriction enzyme digestion to expose diagnostic DNA bands of specific lengths (restriction enzymes were purchased from New England BioLabs), as well as control uncut plasmid to eliminate unwanted multimeric assemblies (**Figure 3g** and **Supplementary Figure 14**). All empty backbone vectors, initial domesticated parts, constitutively expressed luciferase units, and the final multi-luciferase reporter plasmid are available through Addgene (https://www.addgene.org/) (**Supplementary Table 4**). All plasmid maps can be viewed and analyzed using SnapGene software (above) or SnapGene Viewer freeware software (http://www.snapgene.com/products/snapgene_viewer/) (GSL Biotech LLC).

Cell culture

All cell lines used in this study were obtained from the Tissue and Cell Culture Core at Baylor College of Medicine and the Characterized Cell Line Core Facility at MD Anderson, and cultured according to standard mammalian tissue culture protocols and sterile techniques (**Supplementary Table 8**). Cell lines were incubated at 37°C and 5% CO_2. Specific growth media, cellular density, and plate format used for siRNA and luciferase reporter plasmid transfections are summarized for each cell line in **Supplementary Table 8**. For quantitative PCR, cells were plated at a density of 4 x 10^5 cells/well in 6-well plates for RNA extraction. To confirm the identity of all cell lines used in this study, short tandem repeat DNA fingerprinting was performed at the Characterized Cell Line Core Facility (MD Anderson) (**Supplementary Table 9**).

Plasmid and siRNA transfection

Lipofectamine 3000 (Thermo Fisher Scientific) was used for all plasmid transfections. We used the standard transfection protocol indicated in the accompanied manual for plasmids smaller than five kilobases, in a 96-well plate: 100 ng plasmid, 15 μL Opti-MEM (Thermo Fisher Scientific), 0.2 μL P3000 reagent, and 0.2 μL

lipofectamine reagent was used in a total volume of 15.4 μL per sample (with addition of the volume of the DNA) to prepare the DNA-plasmid complexes. We used a modified transfection protocol for plasmids larger than five kilobases: 150 ng plasmid DNA, 15 μL Opti-MEM (Gibco), 0.3 μL, P3000 reagent, and 0.3 μL lipofectamine reagent in a total volume of 15.6 μL per sample (with addition of the volume of the DNA) was used to prepare the DNA-plasmid complexes. When 48-well plates were used, volumes were adjusted proportionally: twice the amounts of all reagents were used per sample to prepare the DNA-plasmid complexes.

Lipofectamine RNAiMAX Reagent (Thermo Fisher Scientific) was used for all siRNA transfections as recommended by the manufacturer. All siRNAs (**Supplementary Table 6**) were purchased from Sigma-Aldrich and transfected at a final concentration of 10 nM. The MISSION® siRNA Universal Negative Control #1 (Sigma-Aldrich) was used as non-targeting siRNA to create a baseline for mRNA knockdown efficiency, and the knockdown potency of all targeting siRNAs were normalized to this negative control.

Measurement of luciferase activities and bioluminescent spectra

Luciferase activities were measured using the CLARIOStar multimode microplate reader (BMG LABTECH GmbH), incorporating appropriate bandpass (BP) filters when necessary. All luciferase emission measurements were performed using the Dual-Luciferase® Reporter assay (DLR™ assay, Promega). At 24 hours post-transfection (with or without treatments as indicated), cells were washed with 150 μL phosphate buffered saline (PBS) per well for 96- or 48-well plates, followed by cell lysis using 40 or 60 μL of Passive Lysis Buffer (PLB) per well for 96- or 48-well plates, respectively. The necessary amount of lysate required for experiments (below) were transferred to white 384-well plates for luminescence recordings.

We recorded full-spectrum luminescence for individual luciferase measurement using the emission Linear Variable Filter (LVF) monochromator of the CLARIOStar multimode microplate reader: bandwidth was set to 10 nm and measurements were taken from 350 to 700 nm in 1 nm steps. Luciferase measurements were initiated 5 seconds after addition of 10 μL of the appropriate buffer (containing appropriate substrate) to 5 μL of the cell lysates: LARII buffer (containing D-Luciferin) alone for the D-Luciferin-responsive luciferases, or followed by the addition of Stop & Glo® Buffer containing quencher and coelenterazine for the coelenterazine-responsive luciferases. The performance of all luciferases was also evaluated by just adding buffer containing quencher

and coelenterazine, without previously adding D-Luciferin-containing buffer. This resulted in luminescence readings lower than the background threshold set for the D-Luciferin luciferases and weaker luminescence readings for the coelenterazine luciferases, compared to the luminescence readings obtained when D-Luciferin-containing buffer is added previously (data not shown). To improve the signal-to-noise ratio, the smoothing algorithm of the MARS Data Analysis Software (BMG Labtech) was applied with a boxcar width set to 9 for all samples. Subsequently, we normalized the data by setting the maximum emission peak at 100%.

For multiplex luciferase recordings, we determined the D-Luciferin luminescence 30 seconds after the addition of 10 μL of LARII buffer (containing D-Luciferin substrate) by measuring **1**) total, **2**) BP515-30-filtered, and **3**) BP530-40-filtered light for 2 seconds each. In a second step, we determined the coelentarazine luminescence 7 seconds after adding 15 μL of Stop & Glo® buffer (containing quencher to annihilate the luminescence from the first step, and coelenterazine substrate) by measuring **1**) BP410-80-filtered, **2**) BP570-100-filtered, and **3**) total light for 1 second each (see **Supplementary Figure 7** for a schematic of the protocol).

Two additional luciferase assay kits, Nano-Glo® luciferase assay (Promega) and Dual-Glo® luciferase assay (Promega), were tested in this study but ultimately not used for the multi-luciferase experiments.

Total protein quantification

The Pierce BCA Protein Assay Kit (Thermo Fisher Scientific) was used to measure the total protein content in cell lysis samples. Reagents were prepared as indicated in the manual, and 1 μL of the cell lysate was mixed with 40 μL of the reagent in a 384 well plate. Absorbance was measured at 562 nm in a CLARIOStar multimode microplate reader, and total protein concentration was determined by comparing to a bovine serum albumin protein standard. Three technical replicates were performed per protein quantification experiment.

RNA extraction, cDNA synthesis, and quantitative PCR (qPCR)

RNA extraction was performed after drug or siRNA treatment for 24 or 48 hours, respectively. Cells were quickly trypsinized, harvested by centrifugation, and pellets were frozen until further processing. RNA was isolated using the Quick-RNA™ MicroPrep kit (Zymo Research) as recommended by the manufacturer, including the optional DNAse treatment. First-strand cDNA synthesis was performed in a 20 μL reaction using 1000 ng of RNA and 4 μL of the qScript cDNA SuperMix (Quantabio). Next, 4 μL of a 1:5 dilution of cDNA was

used for qPCR, combined with 5µL of PerfeCTa SYBR® Green SuperMix (Quantabio), and 1 µL of a 55 µM primer mix (containing both forward and reverse PCR primers) per sample. Quantitative PCR was performed in 384-well qPCR plates (Roche) using the LightCycler® 480 Real-Time PCR instrument (Roche). qPCR data analysis was performed using qbase+ 3.0 software (Biogazelle)[72]. Primers used for qPCR (candidate reference genes and pathway genes) are listed in **Supplementary Table 10**. We used the geNORM algorithm[73] to determine expression stability of candidate reference genes and the optimal number of reference genes (**Supplementary Figure 22a** and **b**).

Data analysis and statistics

All data were analyzed using Excel (below), followed by Prism 7 software (GraphPad) for statistical analysis and graphing. The resulting graphs were then edited for publication using Adobe Illustrator CC (Adobe Creative Cloud). For linear regressions, Prism reports the P-value test from the null hypothesis that the overall slope is zero, and it is calculated from an F test. For qPCR and multiplex luciferase assays, the $\log_2$ fold-change was calculated (see **Supplementary Table 7** for comparison with percent change between samples and fold-change). Statistical significance of the fold-change in qPCR and multiplex luciferase assays was determined by the multiple t-test using the Holm-Sidak method with alpha = 0.05 (*P <0.05, **P < 0.01, ***P < 0.001, and ****P < 0.0001, n.s. is non significant).

Online Excel files for data analysis

1. Calculation of transmission coefficients (**Supplementary Figure 23**).

2. Calculation of simultaneous equations (**Supplementary Figure 24**).

3. Unformatted measurements from a small group of samples (**Supplementary Figure 25**).

4. Unformatted measurements from a large group of samples: 96-well format (**Supplementary Figure 26**).

Data availability

The source data underlying Figs 1b-h, 2b-d, 2f-h, 4b-d, 5b-f, 6b-e, 6g, 6i-l, Supplementary Figs 5b-e, 6b-e, 8b-d, 9b-d, 11b-d, 12b-d, 15a-e, 16a, 16c-g, 17a-d, 18b-d, 19, 20a-d, and Supplementary Tables 1 and 2 are provided as a Source Data file.

References

1. Ediriweera, M. K., Tennekoon, K. H. & Samarakoon, S. R. In vitro assays and techniques utilized in anticancer drug discovery. *J. Appl. Toxicol. JAT* **39**, 38–71 (2019).

2. Westwick, J. K. & Lamerdin, J. E. Improving drug discovery with contextual assays and cellular systems analysis. *Methods Mol. Biol. Clifton NJ* **756**, 61–73 (2011).

3. Taylor, D. L. & Giuliano, K. A. Multiplexed high content screening assays create a systems cell biology approach to drug discovery. *Drug Discov. Today Technol.* **2**, 149–154 (2005).

4. Garvey, C. M. *et al.* A high-content image-based method for quantitatively studying context-dependent cell population dynamics. *Sci. Rep.* **6**, 29752 (2016).

5. Berg, E. L. Phenotypic chemical biology for predicting safety and efficacy. *Drug Discov. Today Technol.* **23**, 53–60 (2017).

6. Michelini, E. *et al.* Spectral-Resolved Gene Technology for Multiplexed Bioluminescence and High-Content Screening. *Anal. Chem.* **80**, 260–267 (2008).

7. Gustafsdottir, S. M. *et al.* Multiplex cytological profiling assay to measure diverse cellular states. *PloS One* **8**, e80999 (2013).

8. Boutros, M., Heigwer, F. & Laufer, C. Microscopy-Based High-Content Screening. *Cell* **163**, 1314–1325 (2015).

9. Gerets, H. H. J., Dhalluin, S. & Atienzar, F. A. Multiplexing cell viability assays. *Methods Mol. Biol. Clifton NJ* **740**, 91–101 (2011).

10. Simoni, Y., Chng, M. H. Y., Li, S., Fehlings, M. & Newell, E. W. Mass cytometry: a powerful tool for dissecting the immune landscape. *Curr. Opin. Immunol.* **51**, 187–196 (2018).

11. Bray, M.-A. *et al.* Cell Painting, a high-content image-based assay for morphological profiling using multiplexed fluorescent dyes. *Nat. Protoc.* **11**, 1757–1774 (2016).

12. Nair, A. K. & Baier, L. J. Using Luciferase Reporter Assays to Identify Functional Variants at Disease-Associated Loci. *Methods Mol. Biol. Clifton NJ* **1706**, 303–319 (2018).

13. Kaskova, Z. M., Tsarkova, A. S. & Yampolsky, I. V. 1001 lights: luciferins, luciferases, their mechanisms of action and applications in chemical analysis, biology and medicine. *Chem Soc Rev* **45**, 6048–6077 (2016).

14. Branchini, B. R. *et al.* A Firefly Luciferase Dual Color Bioluminescence Reporter Assay Using Two Substrates To Simultaneously Monitor Two Gene Expression Events. *Sci. Rep.* **8**, 5990 (2018).

15. Adams, S. T. & Miller, S. C. Beyond D-luciferin: expanding the scope of bioluminescence imaging in vivo. *Curr. Opin. Chem. Biol.* **21**, 112–120 (2014).

16. Nakatsu, T. *et al.* Structural basis for the spectral difference in luciferase bioluminescence. *Nature* **440**, 372–376 (2006).

17. Ohmiya, Y. Simultaneous multicolor luciferase reporter assays for monitoring of multiple genes expressions. *Comb. Chem. High Throughput Screen.* **18**, 937–945 (2015).

18. Nakajima, Y. *et al.* Multicolor luciferase assay system: one-step monitoring of multiple gene expressions with a single substrate. *BioTechniques* **38**, 891–894 (2005).

19. Schagat, T., Gaguio, A. & Kopish, K. Normalizing genetic reporter assays: approaches and considerations for increasing consistency and statistical significance. *Cell Notes* 9–12 (2007).

20. Thorne, N., Inglese, J. & Auld, D. S. Illuminating insights into firefly luciferase and other bioluminescent reporters used in chemical biology. *Chem. Biol.* **17**, 646–657 (2010).

21. Promega. Nano-Glo® Dual-Luciferase® Reporter Assay System Technical Manual No. TM426. *Promega Corp.* (2015).

22. Sherf, B. A., Navarro, S. L., Hannah, R. R. & Wood, K. V. Dual-LuciferaseTM Reporter Assay: An Advanced Co-Reporter Technology Integrating Firefly and Renilla Luciferase Assays. *Promega Notes* **57**, 2–9 (1996).

23. Hampf, M. & Gossen, M. A protocol for combined Photinus and Renilla luciferase quantification compatible with protein assays. *Anal. Biochem.* **356**, 94–99 (2006).

24. Baker, J. M. & Boyce, F. M. High-throughput functional screening using a homemade dual-glow luciferase assay. *J. Vis. Exp. JoVE* (2014). doi:10.3791/50282

25. Sarrion-Perdigones, A. *et al.* GoldenBraid: an iterative cloning system for standardized assembly of reusable genetic modules. *PLoS.ONE.* **6**, e21622 (2011).

26. Sarrion-Perdigones, A. *et al.* GoldenBraid 2.0: a comprehensive DNA assembly framework for plant synthetic biology. *Plant Physiol* **162**, 1618–1631 (2013).

27. Vazquez-Vilar, M. *et al.* GB3.0: a platform for plant bio-design that connects functional DNA elements with associated biological data. *Nucleic Acids Res.* **45**, 2196–2209 (2017).

28. Yew, N. S. *et al.* Optimization of plasmid vectors for high-level expression in lung epithelial cells. *Hum. Gene Ther.* **8**, 575–584 (1997).

29. Feeney, K. A., Putker, M., Brancaccio, M. & O'Neill, J. S. In-depth Characterization of Firefly Luciferase as a Reporter of Circadian Gene Expression in Mammalian Cells. *J. Biol. Rhythms* **31**, 540–550 (2016).

30. Wassman, C. D. *et al.* Computational identification of a transiently open L1/S3 pocket for reactivation of mutant p53. *Nat. Commun.* **4**, 1407 (2013).

31. Eggermont, J. & Proudfoot, N. J. Poly(A) signals and transcriptional pause sites combine to prevent interference between RNA polymerase II promoters. *EMBO J.* **12**, 2539–2548 (1993).

32. Elston, R. & Inman, G. J. Crosstalk between p53 and TGF-β Signalling. *J. Signal Transduct.* **2012**, 294097 (2012).

33. Cui, Y. *et al.* Transforming growth factor-β1 downregulates vascular endothelial growth factor-D expression in human lung fibroblasts via the Jun NH2-terminal kinase signaling pathway. *Mol. Med. Camb. Mass* **20**, 120–134 (2014).

34. Mountain, D. J. H., Singh, M. & Singh, K. Downregulation of VEGF-D expression by interleukin-1beta in cardiac microvascular endothelial cells is mediated by MAPKs and PKCalpha/beta1. *J. Cell. Physiol.* **215**, 337–343 (2008).

35. Künkele, A. *et al.* Pharmacological activation of the p53 pathway by nutlin-3 exerts anti-tumoral effects in medulloblastomas. *Neuro-Oncol.* **14**, 859–869 (2012).

36. Rocha, S., Campbell, K. J., Roche, K. C. & Perkins, N. D. The p53-inhibitor pifithrin-alpha inhibits firefly luciferase activity in vivo and in vitro. *BMC Mol. Biol.* **4**, 9 (2003).

37. Hiraki, M. *et al.* Small-Molecule Reactivation of Mutant p53 to Wild-Type-like p53 through the p53-Hsp40 Regulatory Axis. *Chem. Biol.* **22**, 1206–1216 (2015).

38. Ma, J., Wang, Q., Fei, T., Han, J.-D. J. & Chen, Y.-G. MCP-1 mediates TGF-beta-induced angiogenesis by stimulating vascular smooth muscle cell migration. *Blood* **109**, 987–994 (2007).

39. Seong, G. J. *et al.* TGF-beta-induced interleukin-6 participates in transdifferentiation of human Tenon's fibroblasts to myofibroblasts. *Mol. Vis.* **15**, 2123–2128 (2009).

40. Khatibi, S. *et al.* TGF-β and IL-6 family signalling crosstalk: an integrated model. *Growth Factors Chur Switz.* **35**, 100–124 (2017).

41. Mezzanotte, L. *et al.* Sensitive dual color in vivo bioluminescence imaging using a new red codon optimized firefly luciferase and a green click beetle luciferase. *PloS One* **6**, e19277 (2011).

42. Heise, K., Oppermann, H., Meixensberger, J., Gebhardt, R. & Gaunitz, F. Dual luciferase assay for secreted luciferases based on Gaussia and NanoLuc. *Assay Drug Dev. Technol.* **11**, 244–252 (2013).

43. Mezzanotte, L., An, N., Mol, I. M., Löwik, C. W. G. M. & Kaijzel, E. L. A New Multicolor Bioluminescence Imaging Platform to Investigate NF-κB Activity and Apoptosis in Human Breast Cancer Cells. *PLoS ONE* **9**, e85550 (2014).

44. Kulak, O. & Lum, L. A multiplexed luciferase-based screening platform for interrogating cancer-associated signal transduction in cultured cells. *J. Vis. Exp. JoVE* e50369 (2013). doi:10.3791/50369

45. Maguire, C. A. *et al.* Triple bioluminescence imaging for in vivo monitoring of cellular processes. *Mol. Ther. Nucleic Acids* **2**, e99 (2013).

46. Kaestner, L., Scholz, A. & Lipp, P. Conceptual and technical aspects of transfection and gene delivery. *Bioorg. Med. Chem. Lett.* **25**, 1171–1176 (2015).

47. Hofemeister, H. *et al.* Recombineering, transfection, Western, IP and ChIP methods for protein tagging via gene targeting or BAC transgenesis. *Methods San Diego Calif* **53**, 437–452 (2011).

48. Poser, I. *et al.* BAC TransgeneOmics: a high-throughput method for exploration of protein function in mammals. *Nat. Methods* **5**, 409–415 (2008).

49. Hasse, S., Hyman, A. A. & Sarov, M. TransgeneOmics--A transgenic platform for protein localization based function exploration. *Methods San Diego Calif* **96**, 69–74 (2016).

50. Sadelain, M., Papapetrou, E. P. & Bushman, F. D. Safe harbours for the integration of new DNA in the human genome. *Nat. Rev. Cancer* **12**, 51–58 (2011).

51. Yeh, H.-W. & Ai, H.-W. Development and Applications of Bioluminescent and Chemiluminescent Reporters and Biosensors. *Annu. Rev. Anal. Chem. Palo Alto Calif* **12**, 129–150 (2019).

52. Yao, Z., Zhang, B. S. & Prescher, J. A. Advances in bioluminescence imaging: new probes from old recipes. *Curr. Opin. Chem. Biol.* **45**, 148–156 (2018).

53. Mezzanotte, L., van 't Root, M., Karatas, H., Goun, E. A. & Löwik, C. W. G. M. In Vivo Molecular Bioluminescence Imaging: New Tools and Applications. *Trends Biotechnol.* **35**, 640–652 (2017).

54. Heitman, L. H. *et al.* False positives in a reporter gene assay: identification and synthesis of substituted N-pyridin-2-ylbenzamides as competitive inhibitors of firefly luciferase. *J. Med. Chem.* **51**, 4724–4729 (2008).

55. Bai, H. *et al.* Discovery of a series of 2-phenylnaphthalenes as firefly luciferase inhibitors. 9

56. Wider, D. & Picard, D. Secreted dual reporter assay with Gaussia luciferase and the red fluorescent protein mCherry. *PloS One* **12**, e0189403 (2017).

57. Evans, R. M. & Mangelsdorf, D. J. Nuclear Receptors, RXR, and the Big Bang. *Cell* **157**, 255–266 (2014).

58. Haeusler, R. A., McGraw, T. E. & Accili, D. Biochemical and cellular properties of insulin receptor signalling. *Nat. Rev. Mol. Cell Biol.* **19**, 31–44 (2018).

59. Jensen, S. & Thomsen, A. R. Sensing of RNA viruses: a review of innate immune receptors involved in recognizing RNA virus invasion. *J. Virol.* **86**, 2900–2910 (2012).

60. Schaumberg, K. A. *et al.* Quantitative characterization of genetic parts and circuits for plant synthetic biology. *Nat. Methods* **13**, 94–100 (2016).

61. Nakajima, Y. *et al.* Enhanced beetle luciferase for high-resolution bioluminescence imaging. *PloS One* **5**, e10011 (2010).

62. Villalobos, V. *et al.* Dual-color click beetle luciferase heteroprotein fragment complementation assays. *Chem. Biol.* **17**, 1018–1029 (2010).

63. Liang, Y., Walczak, P. & Bulte, J. W. M. Comparison of red-shifted firefly luciferase Ppy RE9 and conventional Luc2 as bioluminescence imaging reporter genes for in vivo imaging of stem cells. *J. Biomed. Opt.* **17**, 016004 (2012).

64. Branchini, B. R., Southworth, T. L., DeAngelis, J. P., Roda, A. & Michelini, E. Luciferase from the Italian firefly Luciola italica: molecular cloning and expression. *Comp. Biochem. Physiol. B Biochem. Mol. Biol.* **145**, 159–167 (2006).

65. Viviani, V. R., Bechara, E. J. & Ohmiya, Y. Cloning, sequence analysis, and expression of active Phrixothrix railroad-worms luciferases: relationship between bioluminescence spectra and primary structures. *Biochemistry* **38**, 8271–8279 (1999).

66. Hall, M. P. *et al.* Engineered luciferase reporter from a deep sea shrimp utilizing a novel imidazopyrazinone substrate. *ACS Chem. Biol.* **7**, 1848–1857 (2012).

67. Lorenz, W. W., McCann, R. O., Longiaru, M. & Cormier, M. J. Isolation and expression of a cDNA encoding Renilla reniformis luciferase. *Proc. Natl. Acad. Sci. U. S. A.* **88**, 4438–4442 (1991).

68. Markova, S. V., Golz, S., Frank, L. A., Kalthof, B. & Vysotski, E. S. Cloning and expression of cDNA for a luciferase from the marine copepod Metridia longa. A novel secreted bioluminescent reporter enzyme. *J. Biol. Chem.* **279**, 3212–3217 (2004).

69. Invivogen. *Introducing Lucia: a new secreted luciferase - Review.*

70. Tannous, B. A., Kim, D.-E., Fernandez, J. L., Weissleder, R. & Breakefield, X. O. Codon-optimized Gaussia luciferase cDNA for mammalian gene expression in culture and in vivo. *Mol. Ther. J. Am. Soc. Gene Ther.* **11**, 435–443 (2005).

71. Loening, A. M., Wu, A. M. & Gambhir, S. S. Red-shifted Renilla reniformis luciferase variants for imaging in living subjects. *Nat. Methods* **4**, 641–643 (2007).

72. Hellemans, J., Mortier, G., De Paepe, A., Speleman, F. & Vandesompele, J. qBase relative quantification framework and software for management and automated analysis of real-time quantitative PCR data. *Genome Biol.* **8**, R19 (2007).

73. Vandesompele, J. *et al.* Accurate normalization of real-time quantitative RT-PCR data by geometric averaging of multiple internal control genes. *Genome Biol.* **3**, RESEARCH0034 (2002).

End notes

Acknowledgments

Author contributions

A.S-P. and K.J.T.V. conceptualized the study. A.S-P., L.C., D.W.Y., and K.J.T.V. planned and designed the study. A.S-P., L.C., Y.G., and T.G-F. performed experiments. A.S-P., L.C., and Y.G. analyzed the data. A.S-P and K.J.T.V. drafted the manuscript, which was revised according to feedback from all other authors. K.J.T.V. and D.W.Y. supervised the study.

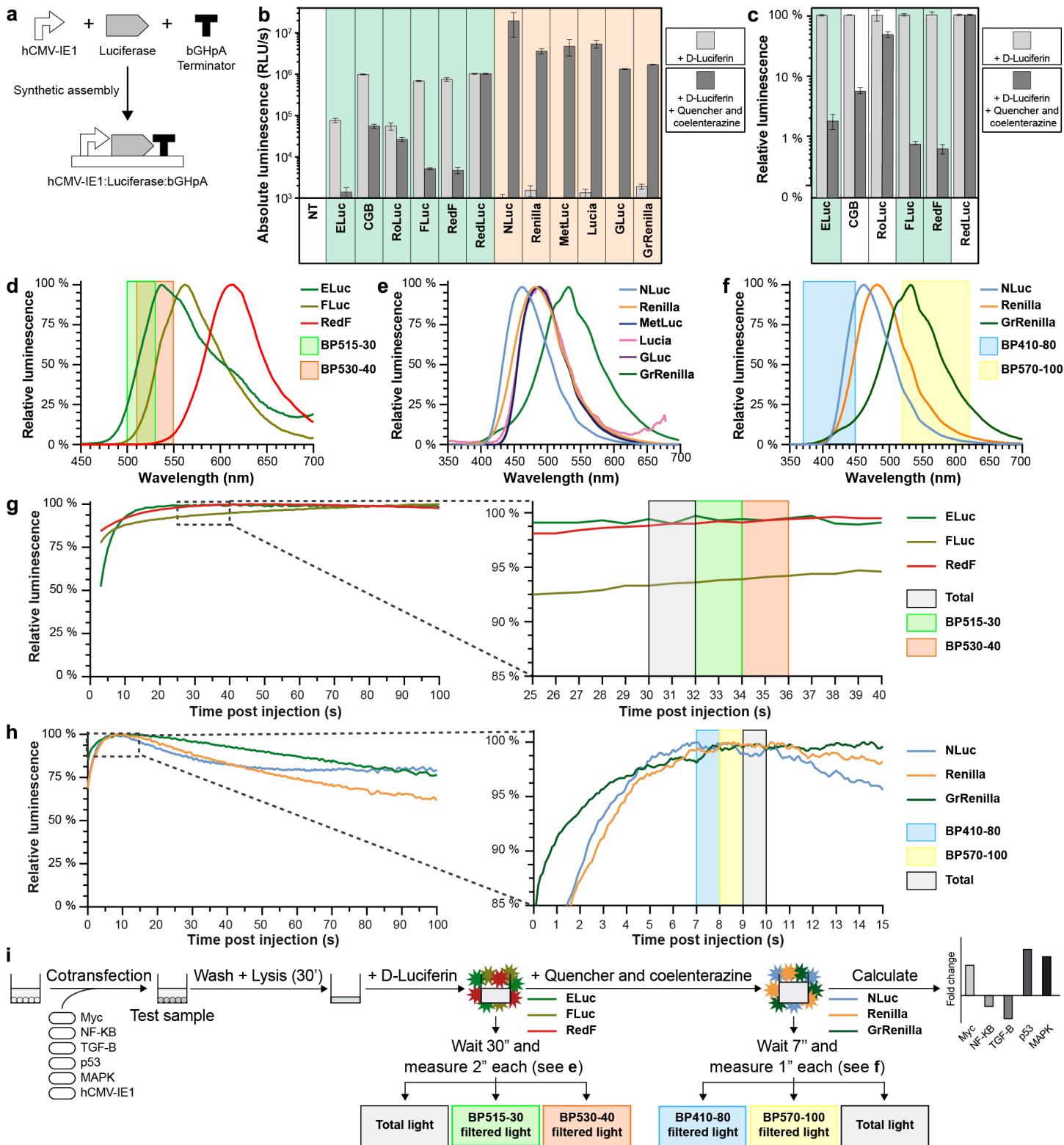## Conflict of interest

No conflicts of interest

Figures and figure legends

Figure 1. Experimental parameters for multiplex hextuple luciferase assaying. (**a**) Simplified schematic of obtaining a constitutively expressed luciferase transcriptional unit by synthetic assembly of three parts:

constitutive hCMV-IE1 promoter, luciferase, and bovine growth hormone polyadenylation (bGHpA) terminator. (**b**) Absolute luminescence emitted by 12 transcriptional luciferase units during both steps of a dual-luciferase assay. Luminescence was recorded after addition of D-Luciferin-containing buffer alone or followed by the addition of a second buffer containing quenching reagent and coelenterazine. RLU/s, relative light units per second. NT, non-transfected control. (**c**) Quenching potency of D-Luciferin-responsive luciferases after addition of D-Luciferin-containing buffer alone or followed by the addition of a second buffer containing luciferase-quenching agent and coelenterazine substrate. To visualize quenching potency for the D-Luciferin-responsive luciferases absolute luminescence measurements (see **b**) are now represented in relative units. (**d**) Emission spectra of three quenchable and spectrally-distinguishable D-Luciferin luciferases. Two bandpass emission filters, one measuring between 500 and 530 nm (BP515-30), and a second measuring between 510 and 550 nm (BP530-40), were used for spectral unmixing, respectively, and are indicated over the spectra. (**e**) Emission spectra of six coelenterazine luciferases. Spectral overlap between Renilla, MetLuc, Lucia, and GLuc, indicate that not all of these can be spectrally distinguished from each other. (**f**) Emission spectra of the three most optimal spectrally-distinguishable coelenterazine luciferases. Two bandpass emission filters, one measuring between 370 and 450 nm (BP410-80), and a second measuring between 520 and 620 nm (BP570-100), were used for the spectral unmixing, respectively, and are indicated over the spectra. (**g**) Determination of the time interval to perform emission measurements after the addition of D-Luciferin. Overlay of the kinetic charts of the three D-Luciferin-responsive luciferases (**Left**) and a close-up of the section between 25 and 40 seconds (**Right**), reveal the three most stable 2-second intervals, 30 seconds post-injection, to perform emission measurements. (**h**) Determination of the time interval to perform emission measurements after the addition of D-Luciferin and the quenching agent and coelenterazine substrate. Overlay of the kinetics of the three coelenterazine luciferases (**Left**) and a close-up window of the section between 0 and 15 seconds (**Right**), reveal the three most stable 1-second intervals, 7 seconds post-injection, to perform emission measurements. (**i**) Schematic of the empirically-determined multiplex hextuple luciferase assay. After cotransfection, cells are incubated for 24 hours. Next, a cell sample is washed, lysed for 30 minutes, and transferred to a plate reader equipped with appropriate bandpass emission filters (**d** and **f**). Then, D-Luciferin substrate is added and three emission measurements are recorded 30 seconds later: total light, BP515-30-filtered light, and BP530-40-filtered light (**g**). Finally, quencher and coelenterazine substrate are added and three additional emission

measurements are recorded 7 seconds later: BP410-80-filtered light, BP570-100-filtered light, and total light (**h**) (**Supplementary Figure 7**). Four technical replicates are included in each data point, and the standard error of the mean is represented (**b** and **c**). Spectra (**d** to **f**) include data from one spectral scan, which was compared with four other technical replicates, and showed no significant changes amongst them. Kinetic charts (**g** to **h**) include data from one biological sample, which was compared with four other technical replicates, and showed no significant changes amongst them. Source data are provided as a Source Data file.
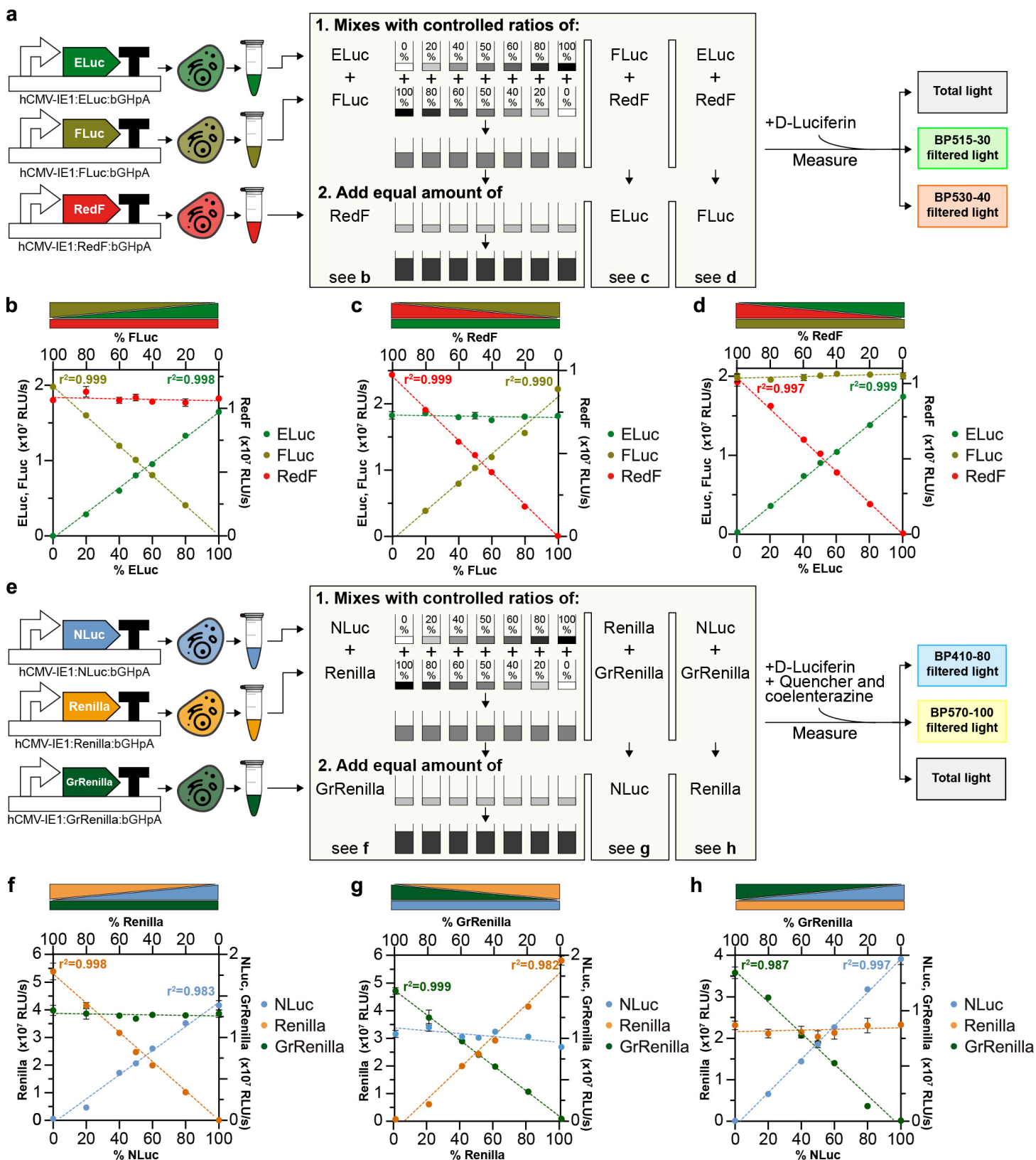
Figure 2. Quantitative determination of dynamic range of luciferase mixtures. (**a**) Schematic of the experimental setup used to confirm the quantitative relationships between the D-Luciferin-responsive

luciferases in a single emission recording experiment. Individual plasmids, each having one transcriptional D-Luciferin-responsive luciferase unit (see **Figure 1a**), were transfected into HEK293T/17 cells. Transfected cells were harvested and lysed after 24 hours. To confirm a quantitative relationship between ELuc and FLuc (**b**), defined amounts of each cell lysate were mixed at different ratios totaling 100% before addition of an equal amount of RedF. After the addition of D-Luciferin substrate, total and filtered light were measured after 30 seconds (**Figure 1g**). Similar experimental setups were used to confirm the quantitative FLuc/RedF (**c**) and ELuc/RedF (**d**) relationships. (**e**) Schematic of the experimental setup used to confirm quantitative relationships between the coelenterazine-responsive luciferases in a single emission recording experiment. Individual plasmids, each having one transcriptional coelenterazine-responsive luciferase unit (see **Figure 1a**), were transfected into HEK293T/17 cells. Transfected cells were harvested and lysed after 24 hours. To confirm a quantitative relationship between NLuc and Renilla (**f**), defined amounts of each cell lysate were mixed at different ratios totaling 100% before addition of an equal amount of GrRenilla. After the addition of quencher and coelenterazine substrate, total and filtered light were measured after 7 seconds (**Figure 1h**). Similar experimental setups were used to determine the quantitative Renilla/GrRenilla (**g**) and NLuc/GrRenilla (**h**) relationships. For **b-d** and **f-h**, P-value < 0.0001 for all regression lines at varying concentrations. For luciferases kept at constant concentration, all minimal slopes that were interpolated by regression did not significantly differ from zero. Four technical replicates are included in each data point, and the standard error of the mean is represented. Source data are provided as a Source Data file.
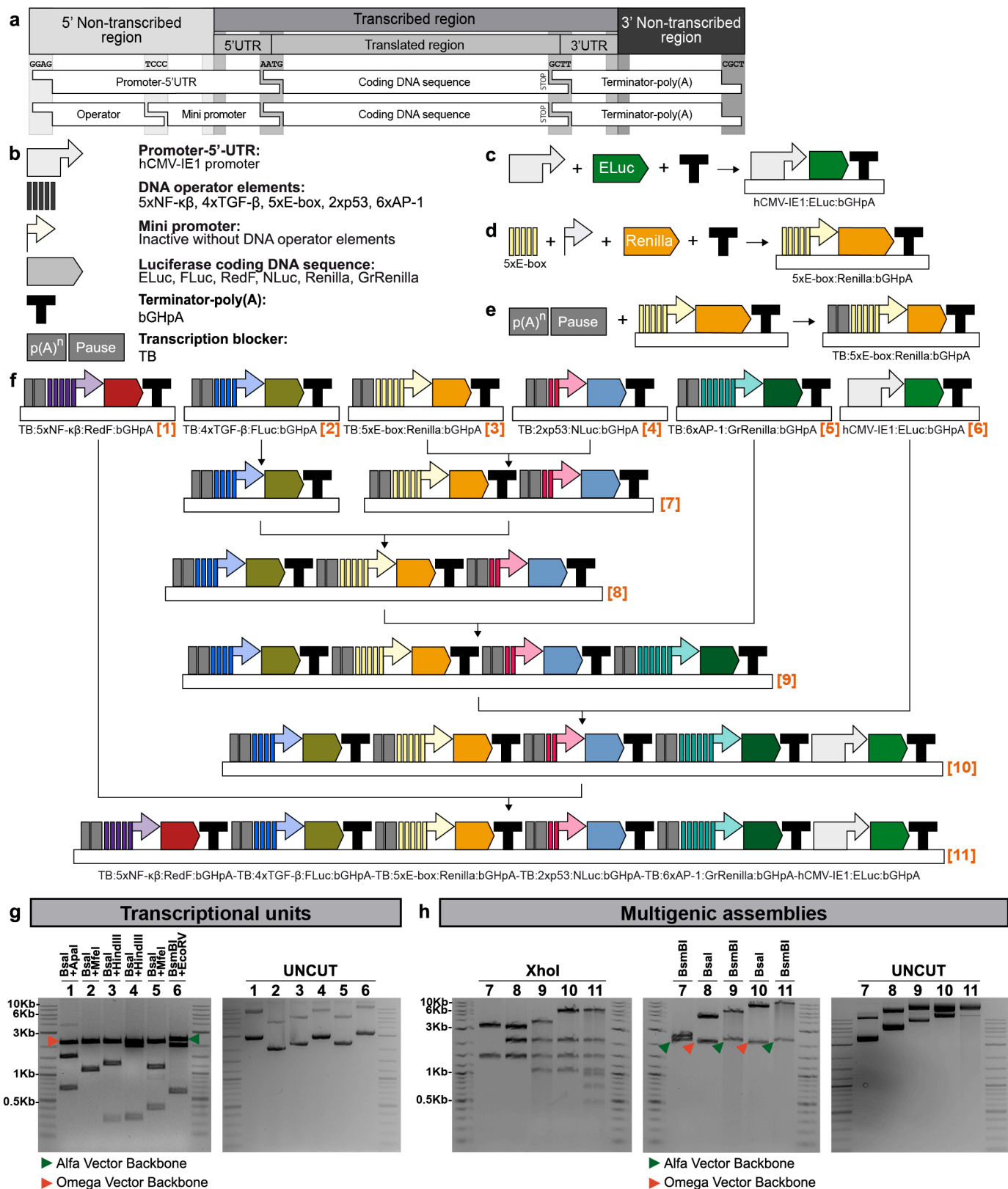
Figure 3. Implementation of synthetic assembly cloning for inserting multiple luciferase reporters into a single vector. (**a**) Schematic of the different DNA element categories. Defined synthetic assembly cloning overhangs generated by BsaI cutting (GGAG, TCCC, AATG, GCTT, and CGCT) allow directional assembly of

pre-made DNA fragments into defined transcriptional units. (**b**) Categories of DNA elements include: (**1**) Full promoter and 5'UTR (cytomegalovirus promoter, hCMV-IE1 promoter) used in all constitutively expressed transcriptional units; (**2**) DNA operator elements (different DNA pathway response elements whose activities are regulated by cellular signaling events, see **Supplementary Table 3**); (**3**) minimal promoter (synthetic minimal TATA-box promoter with low basal activity, mini promoter) needed for transcription initiation driven by the different DNA pathway operator response elements; (**4**) luciferase-coding DNA sequence (see **Table 1**), including codon for translation termination (STOP); (**5**) terminator-poly(A) sequence (terminator of the bovine growth hormone polyadenylation signal, bGHpA); and (**6**) transcription blocker (TB), consisting of a synthetic polyA terminator (p(A)n) and the RNA polymerase II transcriptional pause signal from the human α2 globin gene (Pause), to prevent transcriptional interference between different pathway-responsive luciferase transcriptional units. (**c**) Multipartite assembly of a constitutively expressed luciferase. (**d**) Multipartite assembly of DNA operator elements, minimal promoter, luciferase, and terminator into a pathway-responsive luciferase transcriptional unit. (**e**) Binary assembly of a transcription blocker (TB) upstream of each pathway-responsive unit. (**f**) Overview of the binary assembly steps used to stitch together six luciferase transcriptional units into a single multi-luciferase plasmid using successive bipartite assembly steps. The final multi-luciferase plasmid includes the six luciferase transcriptional units, i.e., five insulated pathway-responsive luciferase transcriptional units and one constitutively expressed luciferase transcriptional unit used as the control for normalization. (**g**) DNA analysis (restriction enzyme fingerprinting and uncut) of all six individual luciferase transcriptional units (Plasmids 1-6), intermediate assemblies (Plasmids 7-10), and final hextuple luciferase vector (Plasmid 11) demonstrates the stability and integrity of all plasmids. Plasmid maps and restriction enzymes used are indicated in **Supplementary Figure 14**. Plasmids encoding DNA building blocks, individual luciferase transcriptional units, and the final multigenic luciferase reporter have been deposited at Addgene (**https://www.addgene.org/**) (**Supplementary Table 4**).
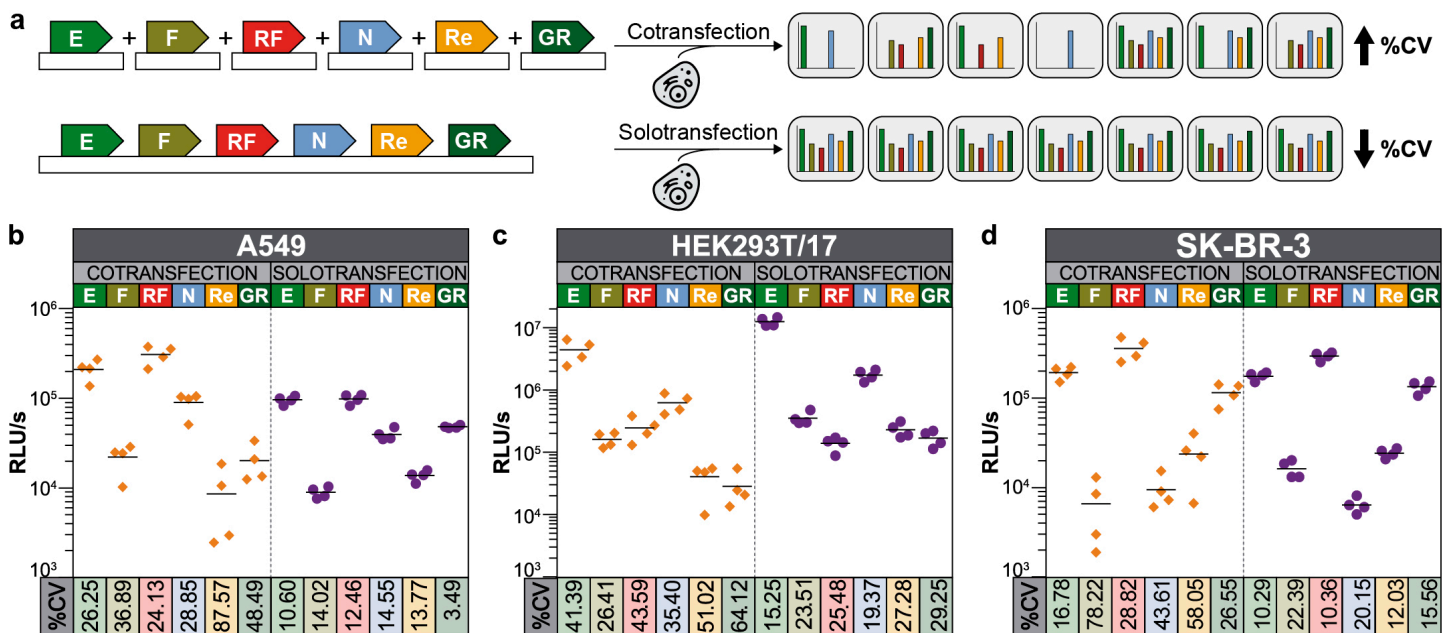
Figure 4. Solotransfection of a single multi-luciferase reporter vector results in lower experimental variability than cotransfection of six individual luciferase reporters. (**a**) Schematic illustrating cellular uptake and variability issues likely encountered during cotransfection of six individual plasmids each encoding a single luciferase transcriptional unit (**Top**). These effects are not observed with solotransfection of a single plasmid encoding all six luciferase transcriptional units (**Bottom**). Equivalent cellular uptake of all luciferase units and a lower coefficient of variation (%CV) were observed with solotransfection, but not with cotransfection. (**b-d**) Variability in the quantification of the different luciferases following cotransfection (**Left**) or solotransfection (**Right**). The absolute luminescence in relative luminescence units per second (RLU/s) of four biological replicates, measured as previously described (**Figure 1i** and **Supplementary Figure 7**), is represented on the y-axis, while the %CV between replicates is indicated on the x-axis for A549 (**b**), HEK293T/17 (**c**), and SK-BR-3 (**d**) cells. A lower %CV was observed during solotransfection, compared to cotransfection, for all luciferase measurements in all three cell lines. E (ELuc), F (FLuc), RF (RedF), N (NLuc), Re (Renilla), GR (GrRenilla). Four technical replicates are included in each data point; the mean is represented with the horizontal bar. Source data are provided as a Source Data file.
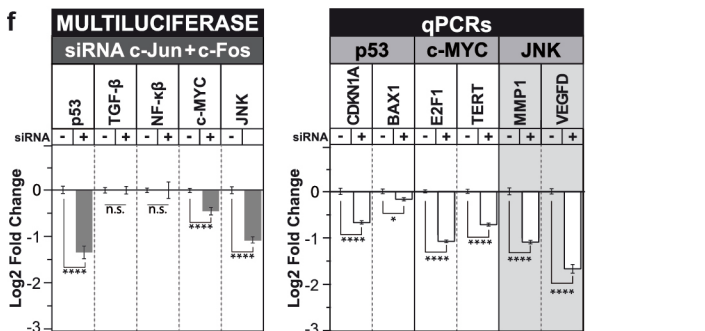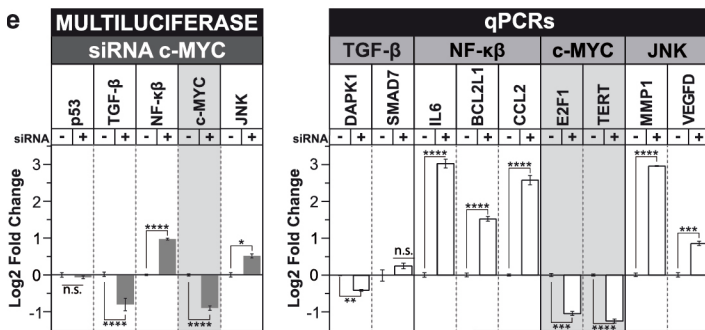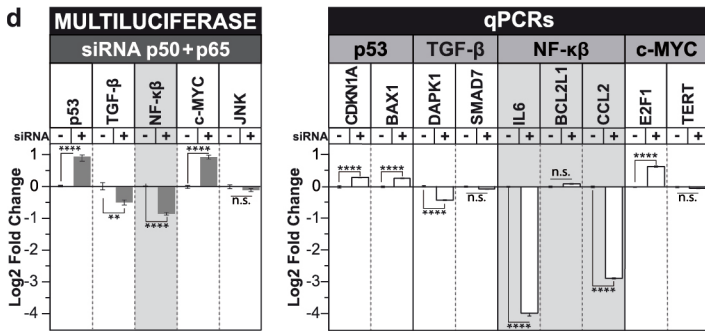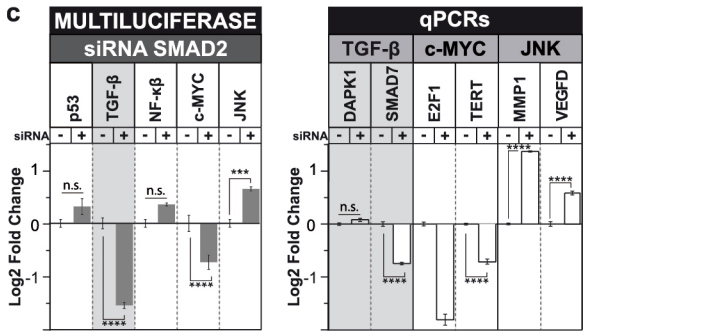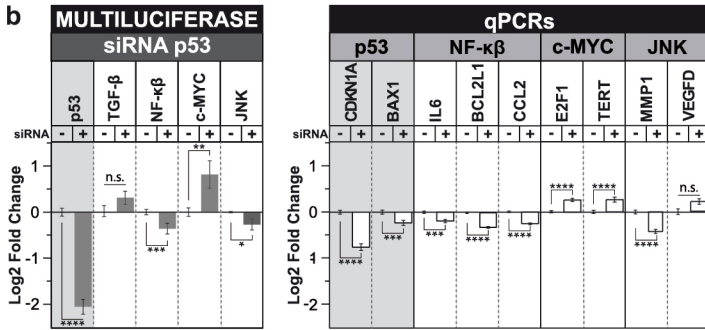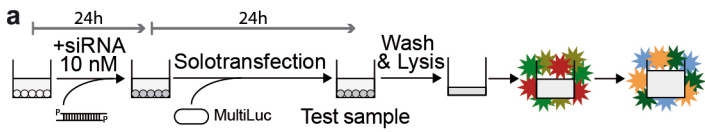
-43-

Figure 5. Multiplex luciferase assaying simultaneously detects the collateral and direct effects of siRNA knockdown of a single pathway. (**a**) A549 cells were treated with 10 nM siRNA and incubated for 24 hours before solotransfection of the multi-luciferase reporter. After another 24 hours, cells were lysed and then the multiplex hextuple luciferase assay and quantitative PCR were performed as described. (**b**) The siRNA silencing of *TP53* effectively reduced p53_RE-regulated luciferase expression and decreased mRNA levels of two TP53 downstream genes, *CDKN1A* and *BAX1*. The multi-luciferase assay revealed collateral downregulation of NF-κβ and MAPK/JNK, as well as upregulation of c-Myc pathway activity, correlating with changes in mRNA levels of downstream target genes associated with each of these pathways. (**c**) The siRNA knockdown of SMAD2 in A549 cells previously stimulated with recombinant TGF-β protein reduced the SMAD2-regulated luciferase expression, as well as knocked down the mRNA expression levels of *SMAD7*, a key downstream target gene of this pathway. Collateral effects observed with this treatment were the downregulation of the c-Myc and upregulation of the MAPK/JNK signaling pathways, which correlated with data on mRNA expression levels of downstream genes obtained by qPCR. (**d**) Downregulation of the NF-κβ pathway through the simultaneous addition of siRNAs targeting *NFKB1* and *RELA* decreased the level of *IL6* and *CCL2* mRNA. Collateral effects observed with this treatment were upregulation of p53 and c-Myc, as well as downregulation of TGF-β pathway activity, that correlated with changes in mRNA expression levels of downstream target genes modulated by these pathways. (**e**) siRNA knockdown of the c-Myc pathway resulted in the reduction of *E2F1* and *TERT* mRNA. Collateral effects observed in this experiment were downregulation of TGF-β, and upregulation of NF-κβ and MAPK/JNK pathway activity, that correlated with changes in mRNA expression levels of several downstream target genes. (**f**) Interfering with the MAPK/JNK pathway through concurrent addition of siRNAs against *JUN* and *FOS* resulted in the reduction of MAPK/JNK pathway activity levels, as well as reduced MMP1 mRNA. Collateral effects observed with this treatment were the simultaneous downregulation of p53 and c-Myc pathway activity that correlated with changes in mRNA expression levels of several downstream target genes regulated by each of these pathways. Statistical significance of the fold-change of different genes analyzed by qPCR and pathways in the multiplex luciferase assay was determined by multiple t-tests using the Holm-Sidak method with alpha = 0.05 (*P <0.05, **P < 0.01, ***P < 0.001, and

****P < 0.0001, n.s. is non-significant). n=4 for both multiplex luciferase assays and qPCR experiments. Source data are provided as a Source Data file.
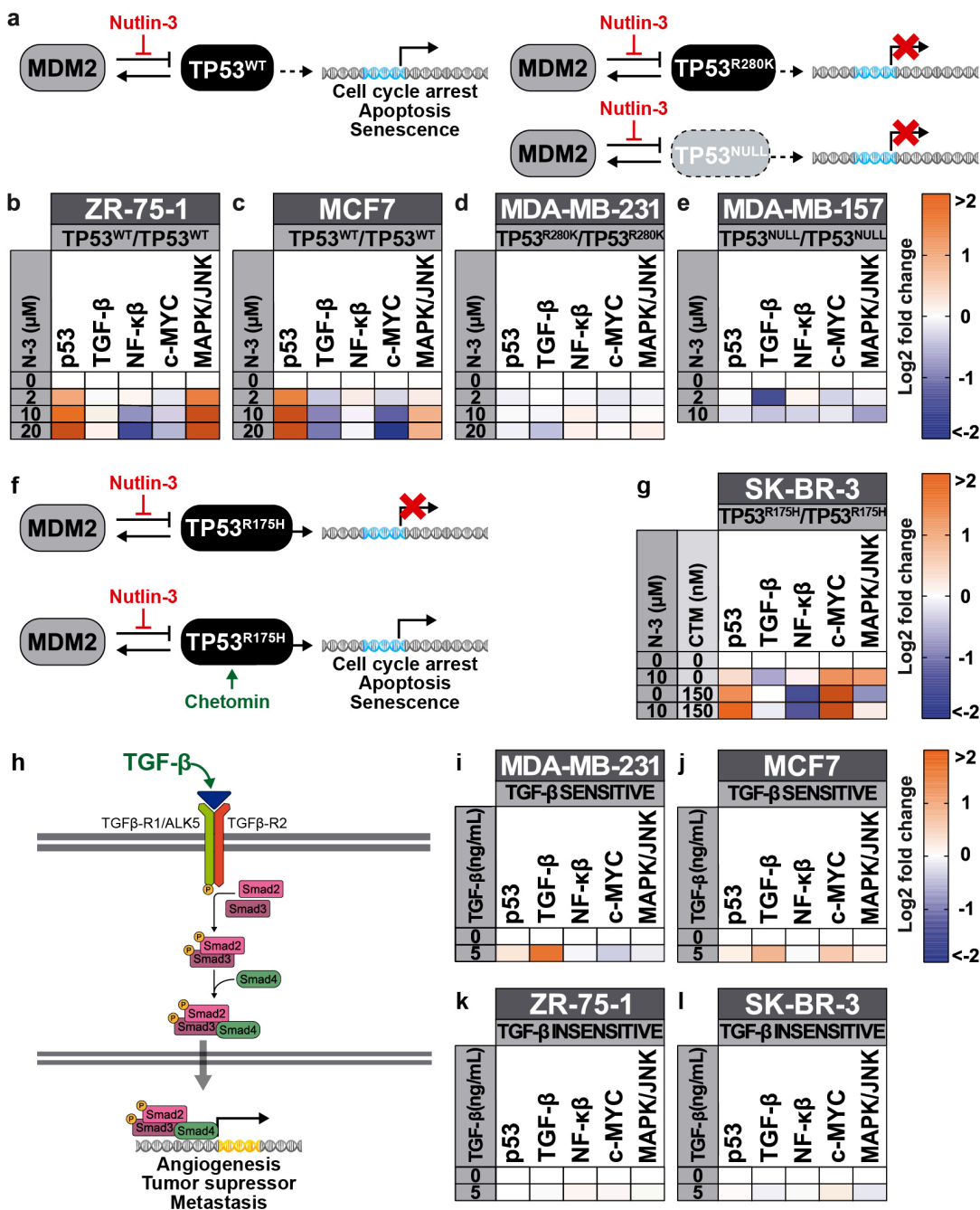
Figure 6. Multiplex luciferase assaying simultaneously detects direct and collateral effects after treatment of breast cancer cell lines with pathway-specific pharmaceuticals or ligands. (**a**) Schematic of p53 pathway activation induced by Nutlin-3. Nutlin-3 selectively inhibits the MDM2-TP53 interaction and activates the p53 pathway in a cell line that expresses wild-type TP53 (TP53^{WT}). Cell lines that express mutant TP53 (TP53^{R280K}) or are p53-deficient (TP53^{NULL}) are resistant to Nutlin-3-induced activation of the p53 pathway. (**b-e**) Heat maps showing the effect of 24-hour treatment with increasing concentrations of Nutlin-3 (N-3) in four breast cancer cell lines: ZR-75-1 (**b**) and MCF7 (**c**) are WT, while MDA-MB-231 is mutant (**d**), and

MDA-MB-157 is null (**e**). The p53 pathway is only activated in the two TP53^{WT} cell lines. Collateral and differential effects across the other pathways examined are shown. (**f**) Schematic of MDM2-p53 pathway reactivation by the pharmaceutical Chetomin. Cell lines that express R175H TP53 mutant protein (TP53^{R175H}) are resistant to Nutlin-3-mediated inhibition of MDM2 and activation of the p53 pathway. In the presence of Chetomin, TP53^{R175H} is reactivated and functionally restored to WT-like levels. (**g**) Heat map demonstrating the complementary effect of Nutlin-3 and Chetomin on p53 signaling. SK-BR-3 cells were not significantly affected by Nutlin-3. The addition of 150 nM of Chetomin reactivates the p53 pathway in the presence and absence of Nutlin-3. Collateral and differential effects on the other pathways are shown for all treatments.. (**h**) Schematic of TGF-β pathway activation by TGF-β ligand. TGF-β activates cellular signaling through the heterodimeric receptor TGF-β-R1/ALK5 and TGF-β-R2, resulting in transcriptional activation of downstream genes mediated by Smad2/Smad3/Smad4. (**i-l**) Effect of a 6-hour treatment with 5 ng/mL of recombinant TGF-β in four breast cancer cell lines: MDA-MB-231 (**i**), MCF7 (**j**), ZR-75-1 (**k**), and SK-BR-3 (**l**). Addition of the ligand resulted in significant activation of the downstream luciferase reporter in TGF-β-sensitive lines (MDA-MB-231 and MCF7). Significant downregulation of the c-Myc pathway was also observed in these cell lines. The addition of the ligand did not result in significant pathway activation in TGF-β-insensitive cell lines (ZR-75-1 and SK-BR-3). n=4 for all multiplex luciferase experiments. Source data are provided as a Source Data file.

Tables

Abbreviation	Full name	Luciferase and origin	Substrate	Emission peak (nm)	Reference
ELuc	Enhanced Beetle Luciferase	Green luciferase from *Pyrearinus termitilluminans*	D-Luciferin	537	[61]
CBG	Click Beetle Green Luciferase	Green luciferase from *Pyrophorus plagiophthalamus*	D-Luciferin	537	[62]
RoLuc	*R. ohbai* Luciferase	Green luciferase from *Rhagophthalmus ohbai*	D-Luciferin	557	[18]
FLuc	Firefly Luciferase	Firefly luciferase from *Photinus pyralis* (luc2 version)	D-Luciferin	562	[63]
RedF	Red Firefly Luciferase	Red mutant S286Y luciferase from *Luciola curciata*	D-Luciferin	614	[64]
RedLuc	*P. hirtus* Red Luciferase	Red luciferase from *Phrixothrix hirtus*	D-Luciferin	617	[65]
NLuc	Nano Luciferase	Directed evolved synthetic NanoLuc luciferase, from *Oplophorus gracilirostris*	Furimazine	462	[66]
Renilla	Renilla Luciferase	Luciferase from *Renilla reniformis*	Coelenterazine	481	[67]
MetLuc	*Metridia* Luciferase	Luciferase from *Metridia longa*	Coelenterazine	482	[68]
Lucia	Lucia Luciferase	Synthetic luciferase from Invivogen	Coelenterazine	486	[69]
GLuc	*Gaussia* Luciferase	Luciferase from *Gaussia princeps*	Coelenterazine	487	[70]
GrRenilla	Green Renilla Luciferase	Synthetic mutant Green Renilla luciferase from *Renilla reniformis*	Coelenterazine	532	[71]

Table 1. List of luciferases evaluated in this study.